NTNU – Trondheim
Norwegian University of
Science and Technology

Interplay Between Supercurrent and Magnetization in Josephson Junctions

Vigdis Toresen

MSc in Physics
Submission date: May 2015
Supervisor: Jacob Rune Wüsthoff Linder, IFY

Norwegian University of Science and Technology
Department of Physics

Abstract

The interplay between ferromagnetic and superconducting order in hybrid structures has in recent years attracted considerable interest due to the rich quantum physics that emerges in such systems in addition to their potential application value in low-temperature spintronics. In this thesis, we aim to investigate how spin-supercurrents and the magnetization configuration in ferromagnetic Josephson junctions interact with each other. This is done in the ballistic limit where one may construct wavefunctions that represent quasiparticle excitations and bound-states that may carry a supercurrent. Combining this with the Landau-Lifshitz-Gilbert equation, we find the contribution from the superconducting correlations to the effective field that determines the time-dependence of the magnetization. We first consider the scattering states for a domain wall ferromagnet in a Josephson junction. Then we consider a simpler model consisting of a ferromagnetic bilayer sandwiched by two superconductors. In the latter case, we show that the superconducting phase difference can be used to switch the magnetization orientation of the free layer. Our results suggest that it is possible to use superconductors to control the ground-state configuration of magnetic spin-valves, which in turn could lead to interesting magnetoresistance-like effects.

Sammendrag

Samspillet mellom ferromagnetisk og superledende orden i hybridstrukturer har de siste årene tiltrukket seg betydelig interesse grunnet den rikholdige kvantefysikken som fremkommer i slike system i tillegg til deres potensielle bruksområder i spintronikk. I denne oppgaven sikter vi på å undersøke hvordan spin-superstrømmer og magnetiseringskonfigurasjonen i ferromagnetiske Josephson overganger påvirker hverandre. Dette gjøres i den ballistiske grensen hvor man kan konstruere bølgefunksjoner som representerer kvasipartikkeleksitasjoner og bundne tilstander som kan lede en superstrøm. Ved å kombinere dette med Landau-Lifshitz-Gilbert ligningen, finner vi bidraget fra de superledende korrelasjonene til det effektive feltet som bestemmer tidsavhengigheten til magnetiseringen. Vi betrakter først spredningstilstandene for en domenevegg-ferromagnet i en Josephson overgang. Deretter ser vi på en enklere model bestående av en tolags ferromagnet inneklemt mellom to superledere. I det siste tilfellet, viser vi at den superledende faseforskjellen kan brukes til å snu magnetiseringretningen i det frie laget. Våre resultater tyder på at det er mulig å kontrollere grunntilstandskonfigurasjonen til magnetiske spinnventiler, noe som kan lede til interessante magnetoresistanseffekter.

Acknowledgements

I would like to thank my supervisor Prof. Jacob Linder for providing valuable guidance and advice throughout my work on this thesis.

Contents

Abbreviations

ABS	**A**ndreev **B**ound **S**tates
BCS	**B**ardeen-**C**ooper-**S**chrieffer
BdG	**B**ogoliubov-**d**e **G**ennes
BTK	**B**londer-**T**inkham-**K**lapwijk
DW	**D**omain **W**all
F or **FM**	**F**erromagnet
LLG	**L**andau-**L**ifshitz-**G**ilbert
N	**N**ormal metal
S or **SC**	**S**uperconductor

Symbols

F	Free energy	(J)
M_s	saturation magnetization	(Am^{-2})
k_F	Fermi wave vector in superconductor	(m^{-1})
q_F	Fermi wave vector in ferromagnet	(m^{-1})
u, v	BCS coherence factors	
T_c	critical temperature	(K)
ϕ, γ	superconductor phase	
Δ	order parameter	(J)
λ	domain wall width	(m)
φ	azimuthal angle of the magnetization orientation	
θ	polar angle of the magnetization orientation	

Chapter 1

Introduction

Hybrid structures of superconductors and ferromagnets provide a venue for investigating the interplay between superconductivity and magnetism, which rarely coexist in bulk materials[1]. The very different and seemingly incompatible properties of these materials nevertheless give rise to a variety of interesting effects near their interfaces [1].

1.1 Coexistence of ferromagnetism and superconductivity

Both ferromagnetism and superconductivity are examples of ordered phases which eschew an explanation in terms of classical physics and can thus be considered macroscopic manifestation of quantum mechanical behaviour. These phases can occur when the system is cooled down below a material-dependent critical transition temperature. While magnetism had been known to exist since ancient times, superconductivity was first discovered in by Heike Kamerlingh Onnes in 1911 [2], who observed the vanishing of resistivity in mercury at 4.2 K. A microscopic theory to described the phenomenom was formulated by Bardeen, Cooper and Schieffer

[1] A range of materials have been shown to be exceptions to this rule including the uranium-based heavy fermion compounds.

in 1957 [3]. A year earlier, Vitaly Ginzburg had considered that superconductivity would be suppressed by interaction with the vector potential of a magnetic field. After the BCS theory was introduced it also became clear how superconductivity would be destroyed by an exchange field. On this basis the relationship between superconductivity and ferromagnetism were long viewed as antagonistic. This picture has been challenged in recent years as it has been demonstrated how these effects can coexist under certain conditions. It is even possible for a material to be ferromagnetic and superconducting at the same time as has been observed in UGe_2 [4] and URhGe [5] amongst others.

Electrons carry both spin and charge. Conventional electronic devices are based on the charge of electrons, while leaving the spin degree of freedom unexploited. The manipulation of the spin degree of freedom is the focus of spintronics [6], which in recent decades has become an active research field. While the first spin transport experiments [7, 8] were conducted in ferromagnet-superconductor bilayers, most of the research done on spintronics has involved spin-polarized resistive currents. Resistance leads to energy loss through Joule heating [9] and dissipation which would be minimized by using supercurrents. The combination of superconductivity and spintronics is currently receiving much attention [10] and offers much new territory to be explored.

The object of this thesis is to investigate the prospect of using supercurrents to control the magnetization in a textured ferromagnet which could potentially find application in low temperature spintronics.

1.2 Outline

We begin by introducing the microscopic theory of superconductivity and ferromagnetism in chapters 2 and 3 respectively. This will serve as background for understanding the phenomena described in chapter 4 on some key aspects of the relevant effects that arise in hybrid structures consisting of superconductors and ferromagnets. Chapter 5 sets up a model for deriving the energies of the bound

states in the junction. Finding these energies is central to our approach as they contribute to the free energy of the system and thus determine the equilibrium configuration. In chapter 6 we will study a bilayer structure of two ferromagnets sandwiched between two superconductors with the aim of obtaining analytical results. Chapter 7 concludes the thesis with a summary and discussion, followed by an outlook on future development.

Chapter 2

Superconductivity

The superconducting state differs radically from a normal metal. The most notable phenomenological manifestations of superconductivity are the vanishing of electrical resistivity and the expulsion of magnetic fields, called the Meißner effect. For type I-superconductor, the expulsion is complete and they are sometimes called perfect diamagnets. Type II-superconductors will for a certain range of field strengths allow for inhomogeneous penetration of magnetic flux lines, forming vortices. Both types are characterized by zero resistivity which has been observed by letting persistent currents flow without attenuation for more than a year.

In this chapter we introduce the microscopic BCS-theory of superconductivity which explains these properties and other experimental facts observed in conventional (low temperature) superconductors. A microscopic theory of high-T_c superconductors is still being sought.

2.1 BCS theory

A microscopic theory of superconductivity was presented in a 1957 paper by John Bardeen, Leon N. Cooper and John R. Schrieffer [3]. The basis of the theory is the existence of an attractive interaction between electrons which under certain conditions dominates the repulsive screened Coulomb interaction. In conventional

(BCS) superconductors, the attractive interaction is due to virtual exchange of phonons, but the mechanism of attraction is not important as the results apply more generally.

The Hamiltonian for the system can in second quantization language be written

$$H - \mu N = \sum_{\mathbf{k}\sigma} \varepsilon_{\mathbf{k}} c^\dagger_{\mathbf{k}\sigma} c_{\mathbf{k}\sigma} + \sum_{\mathbf{k}\mathbf{k}'} V_{\mathbf{k}\mathbf{k}'} c^\dagger_{\mathbf{k}\uparrow} c^\dagger_{-\mathbf{k}\downarrow} c_{-\mathbf{k}'\downarrow} c_{\mathbf{k}'\uparrow} \tag{2.1}$$

, where μ is the chemical potential, which in metals is essentially equivalent to the Fermi energy, and

$$\varepsilon_{\mathbf{k}} \equiv \epsilon_{\mathbf{k}} - \mu = \frac{\hbar^2 \mathbf{k}^2}{2m} - \mu \tag{2.2}$$

Henceforth we write simply H in place of $H - \mu N$.

2.1.1 BCS mean-field theory

The superconducting phase is characterized by a macroscopic number of Cooper pairs and the expectation values of the pair annihilation(creation) operators must be non-zero.

In the *mean-field approximation* we assume that the fluctuations around the expectation value are small, so that we can write

$$c_{-\mathbf{k}\downarrow} c_{\mathbf{k}\uparrow} = \langle c_{-\mathbf{k}\downarrow} c_{\mathbf{k}\uparrow} \rangle + \underbrace{c_{-\mathbf{k}\downarrow} c_{\mathbf{k}\uparrow} - \langle c_{-\mathbf{k}\downarrow} c_{\mathbf{k}\uparrow} \rangle}_{\delta_{\mathbf{k}}}. \tag{2.3}$$

By inserting this into the Hamiltonian (2.1) and keeping only terms up to linear order in the fluctuations, $\delta_{\mathbf{k}}$, we get

$$\begin{aligned} H &= \sum_{\mathbf{k}\sigma} \varepsilon_{\mathbf{k}} c^\dagger_{\mathbf{k}\sigma} c_{\mathbf{k}\sigma} + \sum_{\mathbf{k}\mathbf{k}'} V_{\mathbf{k}\mathbf{k}'} \Big[\langle c_{-\mathbf{k}'\downarrow} c_{\mathbf{k}'\uparrow} \rangle \delta^\dagger_{\mathbf{k}} + \langle c^\dagger_{\mathbf{k}\uparrow} c^\dagger_{-\mathbf{k}\downarrow} \rangle \delta_{\mathbf{k}'} + \langle c^\dagger_{\mathbf{k}\uparrow} c^\dagger_{-\mathbf{k}\downarrow} \rangle \langle c_{-\mathbf{k}'\downarrow} c_{\mathbf{k}'\uparrow} \rangle \Big] \\ &= \sum_{\mathbf{k}\sigma} \varepsilon_{\mathbf{k}} c^\dagger_{\mathbf{k}\sigma} c_{\mathbf{k}\sigma} + \sum_{\mathbf{k}\mathbf{k}'} V_{\mathbf{k}\mathbf{k}'} \Big[\langle c_{-\mathbf{k}'\downarrow} c_{\mathbf{k}'\uparrow} \rangle c^\dagger_{\mathbf{k}\uparrow} c^\dagger_{-\mathbf{k}\downarrow} + \langle c^\dagger_{\mathbf{k}\uparrow} c^\dagger_{-\mathbf{k}\downarrow} \rangle c_{-\mathbf{k}'\downarrow} c_{\mathbf{k}'\uparrow} - \langle c^\dagger_{\mathbf{k}\uparrow} c^\dagger_{-\mathbf{k}\downarrow} \rangle \langle c_{-\mathbf{k}'\downarrow} c_{\mathbf{k}'\uparrow} \rangle \Big]. \end{aligned}$$

This is now an effective one-body Hamiltonian. We can make this clearer by introducing the *pairing potential* defined by

$$\Delta_{\mathbf{k}} \equiv -\sum_{\mathbf{k}'} V_{\mathbf{k}\mathbf{k}'} \langle c_{-\mathbf{k}'\downarrow} c_{\mathbf{k}'\uparrow} \rangle \tag{2.4}$$

as well as the constant $E_0 \equiv \sum_{\mathbf{k}} [\varepsilon_{\mathbf{k}} + \langle c^\dagger_{\mathbf{k}\uparrow} c^\dagger_{-\mathbf{k}\downarrow} \rangle \Delta_{\mathbf{k}}]$.

$$H = E_0 + \sum_{\mathbf{k}\sigma} \varepsilon_{\mathbf{k}} [c^\dagger_{\mathbf{k}\sigma} c_{\mathbf{k}\sigma} - 1] + \sum_{\mathbf{k}} -\left[\Delta_{\mathbf{k}} c^\dagger_{\mathbf{k}\uparrow} c^\dagger_{-\mathbf{k}\downarrow} + \Delta^*_{\mathbf{k}} c_{-\mathbf{k}\downarrow} c_{\mathbf{k}\uparrow}\right] \tag{2.5}$$

By exploiting the fermionic anti-commutation relations (2.8a) and the fact that $\varepsilon_{\mathbf{k}}$ (2.2) is even in momentum we can rewrite the second term as $\sum_{\mathbf{k}} \varepsilon_{\mathbf{k}} [c^\dagger_{\mathbf{k}\uparrow} c_{\mathbf{k}\uparrow} - c^\dagger_{\mathbf{k}\downarrow} c_{\mathbf{k}\downarrow}]$ and use this to emphasize the bilinear form of the mean-field Hamiltonian:

$$H = E_0 + \sum_{\mathbf{k}} \begin{pmatrix} c^\dagger_{\mathbf{k}\uparrow} & c_{\text{-}\mathbf{k}\downarrow} \end{pmatrix} \begin{pmatrix} \varepsilon_{\mathbf{k}} & -\Delta_{\mathbf{k}} \\ -\Delta^*_{\mathbf{k}} & -\varepsilon_{\mathbf{k}} \end{pmatrix} \begin{pmatrix} c_{\mathbf{k}\uparrow} \\ c^\dagger_{\text{-}\mathbf{k}\downarrow} \end{pmatrix}. \tag{2.6}$$

The particle-hole operator $(c_{\mathbf{k}\uparrow}, c^\dagger_{\text{-}\mathbf{k}\downarrow})^T$ is called a *Nambu Spinor*.

2.1.2 Diagonalization of the BCS Hamiltonian

Diagonalization of the effective one-particle Hamiltonian (2.5) is accomplished via the introduction of new fermionic operators

$$\begin{pmatrix} \gamma_{\mathbf{k}\uparrow} \\ \gamma^\dagger_{\text{-}\mathbf{k}\downarrow} \end{pmatrix} = \begin{pmatrix} u^*_{\mathbf{k}} & -v^*_{\mathbf{k}} \\ v_{\mathbf{k}} & u_{\mathbf{k}} \end{pmatrix} \begin{pmatrix} c_{\mathbf{k}\uparrow} \\ c^\dagger_{\text{-}\mathbf{k}\downarrow} \end{pmatrix}. \tag{2.7}$$

In order that this transformation preserve the canonical anti-commutation relations:

$$\{\gamma^\dagger_{\mathbf{k}\sigma}, \gamma_{\mathbf{k}'\sigma'}\} = \{c^\dagger_{\mathbf{k}\sigma}, c_{\mathbf{k}'\sigma'}\} = \delta_{\mathbf{k}\mathbf{k}'}\delta_{\sigma\sigma'} \tag{2.8a}$$

$$\{\gamma^\dagger_{\mathbf{k}\sigma}, \gamma^\dagger_{\mathbf{k}'\sigma'}\} = \{c^\dagger_{\mathbf{k}\sigma}, c^\dagger_{\mathbf{k}'\sigma'}\} = \{\gamma_{\mathbf{k}\sigma}, \gamma_{\mathbf{k}'\sigma'}\} = \{c_{\mathbf{k}\sigma}, c_{\mathbf{k}'\sigma'}\} = 0, \tag{2.8b}$$

we must require that

$$\begin{aligned}\{\gamma_{\mathbf{k}\uparrow}^\dagger, \gamma_{\mathbf{k}\uparrow}\} &= \{u_{\mathbf{k}} c_{\mathbf{k}\uparrow}^\dagger - v_{\mathbf{k}}^* c_{-\mathbf{k}\downarrow}, u_{\mathbf{k}}^* c_{\mathbf{k}\uparrow} - v_{\mathbf{k}} c_{-\mathbf{k}\downarrow}^\dagger\} \\ &= |u_{\mathbf{k}}|^2 \underbrace{\{c_{\mathbf{k}\uparrow}^\dagger, c_{\mathbf{k}\uparrow}\}}_{=1} + |v_{\mathbf{k}}|^2 \underbrace{\{c_{-\mathbf{k}\downarrow}, c_{-\mathbf{k}\downarrow}^\dagger\}}_{=1} - u_{\mathbf{k}}^* v_{\mathbf{k}}^* \underbrace{\{c_{\mathbf{k}\uparrow}, c_{-\mathbf{k}\downarrow}\}}_{=0} - u_{\mathbf{k}} v_{\mathbf{k}} \underbrace{\{c_{-\mathbf{k}\downarrow}^\dagger, c_{\mathbf{k}\uparrow}^\dagger\}}_{=0} \\ &= |u_{\mathbf{k}}|^2 + |v_{\mathbf{k}}|^2 = 1. \end{aligned} \tag{2.9}$$

With this constraint (2.7) is a unitary, canonical transformation called a *Bogoliubov transformation*. The inverse transformation is now given by

$$\begin{pmatrix} c_{\mathbf{k}\uparrow} \\ c_{\mathbf{-k}\downarrow}^\dagger \end{pmatrix} = \begin{pmatrix} u_{\mathbf{k}} & v_{\mathbf{k}}^* \\ -v_{\mathbf{k}} & u_{\mathbf{k}}^* \end{pmatrix} \begin{pmatrix} \gamma_{\mathbf{k}\uparrow} \\ \gamma_{\mathbf{-k}\downarrow}^\dagger \end{pmatrix}. \tag{2.10}$$

This can now be inserted into the Hamiltonian (2.6).

$$H = E_0 + \sum_{\mathbf{k}} \begin{pmatrix} \gamma_{\mathbf{k}\uparrow}^\dagger & \gamma_{\mathbf{-k}\downarrow} \end{pmatrix} \begin{pmatrix} u_{\mathbf{k}}^* & -v_{\mathbf{k}}^* \\ v_{\mathbf{k}} & u_{\mathbf{k}} \end{pmatrix} \begin{pmatrix} \varepsilon_{\mathbf{k}} & -\Delta_{\mathbf{k}} \\ -\Delta_{\mathbf{k}}^* & -\varepsilon_{\mathbf{k}} \end{pmatrix} \begin{pmatrix} u_{\mathbf{k}} & v_{\mathbf{k}}^* \\ -v_{\mathbf{k}} & u_{\mathbf{k}}^* \end{pmatrix} \begin{pmatrix} \gamma_{\mathbf{k}\uparrow} \\ \gamma_{\mathbf{-k}\downarrow}^\dagger \end{pmatrix} \tag{2.11}$$

The matrix product in the above equation is

$$\begin{pmatrix} \varepsilon_{\mathbf{k}}(|u_{\mathbf{k}}|^2 - |v_{\mathbf{k}}|^2) + (\Delta_{\mathbf{k}} u_{\mathbf{k}}^* v_{\mathbf{k}} + \text{c.c.}) & 2\varepsilon_{\mathbf{k}} u_{\mathbf{k}}^* v_{\mathbf{k}}^* + \Delta_{\mathbf{k}}^* (v_{\mathbf{k}}^*)^2 - \Delta_{\mathbf{k}} (u_{\mathbf{k}}^*)^2 \\ 2\varepsilon_{\mathbf{k}} u_{\mathbf{k}} v_{\mathbf{k}} + \Delta_{\mathbf{k}} v_{\mathbf{k}}^2 - \Delta_{\mathbf{k}}^* u_{\mathbf{k}}^2 & -\varepsilon_{\mathbf{k}}(|u_{\mathbf{k}}|^2 - |v_{\mathbf{k}}|^2) - (\Delta_{\mathbf{k}} u_{\mathbf{k}}^* v_{\mathbf{k}} + \text{c.c.}) \end{pmatrix} \tag{2.12}$$

The off-diagonal terms disappear if we impose the constraint $2\varepsilon_{\mathbf{k}} u_{\mathbf{k}} v_{\mathbf{k}} = \Delta_{\mathbf{k}}^* u_{\mathbf{k}}^2 - \Delta_{\mathbf{k}} v_{\mathbf{k}}^2$. The real and imaginary parts of this equation together with the unitarity condition (2.9) reduce the degrees of freedom for choosing the coefficients $u_{\mathbf{k}}$ and $v_{\mathbf{k}}$ from four to one. The remaining degree of freedom allows us to multiply $u_{\mathbf{k}}$ and $v_{\mathbf{k}}$ by a common phase factor, $\varphi_{\mathbf{k}}$. We fulfill the unitarity condition (2.9) with the parameterization

$$u_{\mathbf{k}} = \mathrm{e}^{i(\varphi_{\mathbf{k}} + \phi_{\mathbf{k}})} \cos\theta_{\mathbf{k}}, \quad v_{\mathbf{k}} = \mathrm{e}^{i(\varphi_{\mathbf{k}} - \phi_{\mathbf{k}})} \sin\theta_{\mathbf{k}}, \quad \Delta_{\mathbf{k}} = |\Delta_{\mathbf{k}}| \mathrm{e}^{i\gamma_{\mathbf{k}}}.$$

The diagonalization constraint then requires the phase of the product $u_{\mathbf{k}} v_{\mathbf{k}}$ to equal the phase of the pairing potential (i.e. $\phi_{\mathbf{k}} = \gamma_{\mathbf{k}}/2$), while the real parameter

$\theta_{\mathbf{k}}$ must satisfy $\tan\theta_{\mathbf{k}} = |\Delta_{\mathbf{k}}|/\varepsilon_{\mathbf{k}}$. The use of some trigonometric identities then reveals

$$|u_{\mathbf{k}}|^2 = \frac{1}{2}\left(1 + \frac{\varepsilon_{\mathbf{k}}}{\sqrt{\varepsilon_{\mathbf{k}}^2 + |\Delta_{\mathbf{k}}|^2}}\right) \tag{2.13a}$$

$$|v_{\mathbf{k}}|^2 = \frac{1}{2}\left(1 - \frac{\varepsilon_{\mathbf{k}}}{\sqrt{\varepsilon_{\mathbf{k}}^2 + |\Delta_{\mathbf{k}}|^2}}\right). \tag{2.13b}$$

.

The resulting Hamiltonian is that of a free fermion quasiparticle gas

$$H = E_0 + \sum_{\mathbf{k}} E_{\mathbf{k}}(\gamma^\dagger_{\mathbf{k}\uparrow}\gamma_{\mathbf{k}\uparrow} - \gamma^\dagger_{\text{-}\mathbf{k}\downarrow}\gamma_{\text{-}\mathbf{k}\downarrow}), \tag{2.14}$$

with dispersion relation

$$E_{\mathbf{k}} = \sqrt{\varepsilon_{\mathbf{k}}^2 + |\Delta_{\mathbf{k}}|^2} \tag{2.15}$$

The dispersion relation reveals the role of $|\Delta_{\mathbf{k}}|$ as a gap in the quasiparticle excitation spectrum. This *energy gap* makes the BCS ground state stable.

2.1.3 Bogolons

The quasiparticles, sometimes called *bogolons*, They are mostly electron(hole)-like far above (below) the Fermi surface. Only close to the Fermi surface do the bogolons consist of electrons and holes of comparable amplitudes. We recover the normal state in the limit $\Delta_{\mathbf{k}} \to 0$. Then the dispersion (2.15) is simply $|\varepsilon_{\mathbf{k}}|$ and (2.13) reduces to

$$|u_{\mathbf{k}}|^2 = \frac{1}{2}\left(1 + \frac{\varepsilon_{\mathbf{k}}}{|\varepsilon_{\mathbf{k}}|}\right) = \begin{cases} 1 & \text{if } \varepsilon_{\mathbf{k}} > 0 \\ 0 & \text{if } \varepsilon_{\mathbf{k}} < 0 \end{cases} \tag{2.16a}$$

$$|v_{\mathbf{k}}|^2 = \frac{1}{2}\left(1 - \frac{\varepsilon_{\mathbf{k}}}{|\varepsilon_{\mathbf{k}}|}\right) = \begin{cases} 0 & \text{if } \varepsilon_{\mathbf{k}} > 0 \\ 1 & \text{if } \varepsilon_{\mathbf{k}} < 0 \end{cases} \tag{2.16b}$$

We see that in the normal state the quasiparticles created are electrons (holes) for energies above (below) the Fermi energy.

2.1.4 Bogoliubov-de Gennes equations

The Bogoliubov-de Gennes (BdG) equations [11] generalize the BCS formalism to treat superconductors with spatially varying pairing strength $\Delta(x)$, chemical potential $\mu(x)$, and Hartree potential $V(x)$.

In the ballstic limit when spin-flip processes can be neglected, the time-evolution of the quasiparticle state is determined by

$$i\hbar\frac{\partial}{\partial t}\begin{pmatrix} u(x) \\ v(x) \end{pmatrix} = \begin{pmatrix} H(x) & \Delta(x) \\ \Delta^*(x) & -H^*(x) \end{pmatrix}\begin{pmatrix} u(x) \\ v(x) \end{pmatrix} \tag{2.17}$$

where

$$H(x) = \frac{1}{2m}(-i\hbar\nabla - \tfrac{e}{c}\mathbf{A}(x))^2 - \mu(x) + V(x). \tag{2.18}$$

Where x is simply the spatial coordinate. The pairing potential $\Delta(x)$ has to be determined self-consistently, although this will not be our task here.

Chapter 3

Ferromagnetism

Micromagnetism describes magnetism at a length scale that is large enough to make the continuum approximation and consider the magnetization as the average of many magnetic moments instead of considering the individual spins separately. At the same time the scale is fine enough to resolve the individual domains of a ferromagnet.

3.1 Free energy of a ferromagnet

The main contributions to the free energy of a ferromagnet include exchange energy, anisotropy energy and magnetostatic energy. All of these interactions tend to align the spin in the same direction. When a macroscopic number of spins point in the same direction, a stray field will form. In order to minimize the stray field, it may be energetically favourable for the ferromagnets to split into domains. The regions between such domains are called domain walls. In the next section we will show how to find the shape of such a wall in the kinds of systems we are considering.

The equilibrium magnetization is found by varying the free energy functional of the system. This gives the effective field

$$\mathbf{H_{eff}} = -\frac{\delta F}{\delta \mathbf{M}}, \tag{3.1}$$

which plays a central role in the dynamics of the magnetization.

3.2 Equilibrium magnetization in a nanowire

We will consider a system with no external field where the main contributions to the free energy comes from exchange interactions and anisotropy. The magnitude of $\mathbf{M}(x)$ is the saturation magnetization, M_s, which does not depend upon x. We define the unit direction vector

$$\mathbf{m}(x) = \frac{\mathbf{M}(x)}{M_s}. \tag{3.2}$$

It will be useful to express $\mathbf{m}(x)$ in Cartesian as well as spherical coordinates

$$\mathbf{m}(x) = \begin{pmatrix} m_x \\ m_y \\ m_z \end{pmatrix} = \begin{pmatrix} \cos\varphi \sin\theta \\ \sin\varphi \sin\theta \\ \cos\theta \end{pmatrix}. \tag{3.3}$$

A magnetization along the wire could produce an important magnetic field in the superconductor. We choose an easy axis along the z-axis and hard axis along the x-axis.

The free energy per area for this system is

$$\mathcal{F} = \int \mathrm{d}x \Big[A(\partial_x \mathbf{m})^2 - K m_z^2 + K_\perp m_x^2 \Big], \tag{3.4}$$

where A is the exchange stiffness and K and $K_\perp$ are anisotropy constants. We assume that $K_\perp \ll K$.

With $\mathbf{m}$ expressed in spherical coordinates we have up to a constant

$$\mathcal{F} = \int \mathrm{d}x \Big[A(\partial_x\theta)^2 + A\sin^2\theta(\partial_x\varphi)^2 + \sin^2\theta(K + K_\perp\cos^2\varphi) \Big]. \tag{3.5}$$

A stationary configuration fulfills the Euler−Lagrange (EL) equations

$$\frac{\delta\mathcal{F}}{\delta\theta} = \sin 2\theta \Big[A(\partial_x\varphi)^2 + K + K_\perp\cos^2\varphi \Big] - 2A\partial_x^2\theta = 0, \tag{3.6}$$

$$\frac{\delta\mathcal{F}}{\delta\varphi} = -\sin^2\theta \Big[K_\perp \sin 2\varphi + 2A\partial_x^2\varphi + 4A\cot\theta(\partial_x\theta)(\partial_x\varphi) \Big] = 0. \tag{3.7}$$

If we assume φ is independent of x (i.e. $\partial_x\varphi = 0$), the EL equation for φ reduces to $\sin 2\varphi = 0$. The stable configuration has $\varphi = \pm\frac{\pi}{2}$, which means the DW lies wholly in the yz-plane (i.e. perpendicular to the hard axis). The EL equation for θ becomes $\partial_x^2\theta = \frac{1}{\lambda^2}\sin\theta\cos\theta$, where we have introduced the *domain wall width* $\lambda = \sqrt{\frac{A}{K}}$. We exploit that $\partial_\theta(\partial_x\theta)^2 = 2\partial_x^2\theta$ and obtain $(\partial_x\theta)^2 = \frac{1}{\lambda^2}\sin^2\theta + \text{const}$.

To determine the integration constant we must specify the boundary conditions. We imagine a semi-infinite ferromagnet where the magnetization (3.2) is homogeneous far from the domain wall (DW) and goes from pointing along $-\hat{z}$ at $-\infty$ to $+\hat{z}$ at $+\infty$. This gives the boundary conditions

$$\lim_{x\to\pm\infty}\partial_x\theta = 0, \qquad \lim_{x\to\pm\infty}\cos\theta = \pm 1. \tag{3.8}$$

This is satisfied by $\partial_x\theta = -\frac{1}{\lambda}\sin\theta$. By separation of variables, we get

$$\begin{aligned} x &= -\lambda\int\frac{\mathrm{d}\theta}{\sin\theta} = -\lambda\int\frac{2i\,\mathrm{e}^{i\theta}\,\mathrm{d}\theta}{\mathrm{e}^{2i\theta}-1} = -\lambda\int\frac{2\mathrm{d}u}{u^2-1} \\ &= -\lambda\ln\frac{u-1}{u+1} + X + i\pi\lambda = -\lambda\ln\tan\tfrac{\theta}{2} + X \end{aligned} \tag{3.9}$$

The integration constant, X, has a physical interpretation as the center of mass (CM) of the DW. Solving for $\theta(x)$ we get

$$\theta(x) = 2 \arctan \exp(-\tfrac{x-X}{\lambda}). \tag{3.10}$$

By inserting (3.10) into (3.2) with $\varphi = \pm\frac{\pi}{2}$ we see that the equilibrium shape of the domain wall is $\mathbf{m}(x) = (0, \pm \operatorname{sech}(\frac{x-X}{\lambda}), \tanh(\frac{x-X}{\lambda}))^T$. The magnetization turns in the plane of the wall. This is called a Néel wall or transverse wall.

Later on we want to consider a slow time dependence of X and φ[1]. In anticipation of this we reinstate an arbitrary φ and the magnetization becomes

$$\mathbf{m}(x) = \begin{pmatrix} \cos\varphi \operatorname{sech}(\frac{x-X}{\lambda}) \\ \sin\varphi \operatorname{sech}(\frac{x-X}{\lambda}) \\ \tanh(\frac{x-X}{\lambda}) \end{pmatrix}. \tag{3.11}$$

3.3 Magnetization Dynamics

The motion of the magnetization in a solid is described by the Landau-Lifshitz-Gilbert equation [12]

$$\frac{\partial \mathbf{m}}{\partial t} = \gamma \mathbf{m} \times \mathbf{H}_{\mathbf{eff}} + \alpha \mathbf{m} \times \frac{\partial \mathbf{m}}{\partial t}, \tag{3.12}$$

where γ is the gyromagnetic ratio and α is the Gilbert damping constant. By the use of an identity from vector calculus, the LLG equation can be shown to be mathematically equivalent to the earlier Landau-Lifshitz equation,

$$\frac{\partial \mathbf{m}}{\partial t} = \gamma \mathbf{m} \times \mathbf{H}_{\mathbf{eff}} - \lambda \mathbf{m} \times \mathbf{m} \times \mathbf{H}_{\mathbf{eff}}, \tag{3.13}$$

which clearly shows that the magnetization will be at rest when it is aligned with the effective field.

[1] For the equilibrium solution to remain valid, φ must stay close to its value at the minimum. It is thus safe to assume that $K \gg K_\perp \cos^2\varphi$ so that the time dependence of λ can be neglected.

Chapter 4

Hybrid structures

When materials with different long-range order are placed in good contact, new physical phenomena can arise at their interface. The Cooper pairs from superconductor will leak into a nearby normal metal where they can survive over considerable lengths. This is called the proximity effect. A similar effect occurs in superconductor/ferromagnet junction [1], though the penetration length is much shorter due to the pair breaking effect of the exchange field. While in an S/N-junction the pair amplitude decays monotonically, in an S/F-junction it oscillates as will be explained below.

4.1 Josephson effect

The Josephson effect [13] is the phenomenon that a current can flow through a nonsuperconducting junction even in the absence of a voltage bias. At finite temperature , the equilibrium current I in a Josephson junction is found by differentiating the free energy F of the junction with respect to the phase difference ϕ between the two superconductors

$$I(\phi) = \frac{2e}{\hbar}\frac{\partial F}{\partial \phi} \tag{4.1}$$

4.2 Andreev reflection

Transmission of an electron with energy less than the superconductor gap from a normal (N) metal through an interface to a superconductor (S) is forbidden to the absence of available quasiparticle states. In order for charge to be conserved when an incident electron from the N side impinges on the barrier to a superconductor, it will be reflected as a hole while a Cooper pair is generated in the superconductor. This process is called Andreev reflection as it was discovered by Alexandr Andreev in 1964 [14].

4.3 Proximity effect in superconductor/ferromagnet junctions

A conventional Cooper pair consists of two electrons with momenta on the opposite side of the Fermi surface in a singlet state. We can write this state as

$$\frac{1}{\sqrt{2}}(|\uparrow,\mathbf{k}\rangle|\downarrow,-\mathbf{k}\rangle - |\downarrow,\mathbf{k}\rangle|\uparrow,-\mathbf{k}\rangle) \tag{4.2}$$

In a ferromagnet, the electronic bands for spin-up and spin-down are split by an amount $2E_{ex}$. Consequently a Cooper pair acquires a center-of-mass momentum, leading to an inhomogeneous phase where the pair amplitude is oscillates with wavenumber corresponding to the CM momentum. This is called a FFLO phase as it was independently discovered in 1964 by Peter Fulde and Richard Ferrell [15] and by Anatoly Larkin and Yurii Ovchinnikov [16]. The oscillations do not penetrate far into the ferromagnetic region because the Zeeman field in the ferromagnet tends to align the spins and thereby breaking up the singlet state [1].

4.4 Induced spin-triplet pairing

Long range superconducting correlations in a ferromagnet requires that the Cooper pairs are formed by electrons of equal spin. The pair correlation function is required to be antisymmetric with respect to interchanging two fermions in order to obey the Pauli exclusion principle [17]. The conventional pairing for the Cooper pairs in BCS-theory is an s-wave spin singlet that is even in momentum and Matsubara frequency. Yet as long as the overall symmetry is odd, several other possibilities are allowed as described in [18]. One example of which is the odd triplet pairing which is odd in frequency with s-wave equal-spin triplet pairing (see review [19]). The equal-spin Cooper pairs are not broken apart by the exchange field and can penetrate up to hundreds of nanometer into a ferromagnet [20]. This remains valid even if the ferromagnet is a half-metal where only one spin conductance channel is available [21, 22]. For an explanation on how triplet pairing can be induced in a conventional singlet superconductor junction containing a textured ferromagnet or spin-active barriers, see [23] or [10].

4.5 Spin-transfer torque

A spin-polarized current carries angular momentum which can affect the orientation of the magnetization in a ferromagnet [24–26]. This phenomenon is called a *spin-transfer torque* after Slonczewski [27]. In the case of resistive currents, this effect has been devoted much attention (see e.g. [28] for a review on current-driven domain wall motion). Also the case of magnetization dynamics with supercurrent has been studied in several works [29–32]. Yet more work needs to be done to clarify how the Andreev bound state spectrum can be used to derive the interplay between superconducting phase difference ϕ and the magnetization orientation [33]. The relationship is complicated as they have a feedback effect on each other [34]. We come back to this in chapter 6 after we have seen how to find the Andreev bound states.

Chapter 5

Andreev bound states

The purpose of this chapter is to show how find the energy levels of the Andreev bound states (ABS) in a superconductor/ferromagnet/superconductor (S/F/S) junction in the ballistic limit of low impurity density. Here we define the mathematical model of the system and present the formalism in the context of our model.

We assume that the characteristic time for the magnetization to vary, is long compared to the time scale of the scattering problem ($\tau_m \gg \hbar\Delta_0^{-1}$). We can therefor regard the system as time independent while we determine the ABS energies. In other words, we are considering an adiabatically changing magnetization such that the system is considered to be in a quasi-equilibrium state at all times.

5.1 Blonder-Tinkham-Klapwijk theory

We derive the ABS energies in a scattering framework, using the BdG equations to treat transmission and reflection at the interfaces. This approach is known as the Blonder-Tinkham-Klapwijk (BTK) theory [35] and was originally applied to transport through an N/S interface. It has since been extended by several authors to encompass various effects in F/S junctions [36, 37]. .

The BTK model is named after G.E. Blonder, M. Tinkham and T.M. Klapwijk who in 1982 [35] presented a unified treatment of transport through a N/S.

While most earlier work had relied on the transfer Hamiltonian, BTK applied the scattering formalism, using the BdG-equations to treat the transmission and reflection of particles at N-S interface [35]. By including a potential barrier of arbitrary strength at the interface encompassing both the tunneling and the metallic limits, as well as the intermediate regime.

5.2 Model and formalism

We consider an S/F/S-junction of width L parallel to the x-axis. The ferromagnetic region contains a domain wall. The leads are conventional s-wave singlet superconducting electrodes. The leads are isotropic in the yz-plane. We assume that the wavefunction is separable and that the nontrivial spatial variation is confined to the x-axis. The y- and z-dependence can then be factored out of the wavefunction

$$\Psi(\mathbf{r}) = \Psi(x)\, \mathrm{e}^{i(k_y y + k_z z)} \tag{5.1}$$

We will omit the trivial y- and z-dependence and treat the system as effectively one-dimensional and let

$$k_F \to \sqrt{k_F^2 - k_y^2 - k_z^2}. \tag{5.2}$$

5.2.1 Basis and notation

Since spin-flip processes can occur at the interfaces it is necessary to consider the full spin⊗Nambu (particle-hole) space and a four-component wave function $\Psi(x) = (u_\uparrow(x), u_\downarrow(x), v_\uparrow(x), v_\downarrow(x))^T$ which represents the state

$$|\Psi(x)\rangle = \sum_\sigma [u_\sigma(x)|e\rangle + v_\sigma(x)|h\rangle] \otimes |\sigma\rangle, \tag{5.3}$$

where $\{e, h\}$ is the particle-hole index and $\sigma \in \{\uparrow, \downarrow\}$ is the spin index, giving the spin-orientation with respect to the quantization axis, which we take to be the z-axis.

We use boldface letters to denote 3-vectors, an arrow above 2-vectors and put a hat on 2x2-matrices. We denote the Pauli matrices with $\hat{\sigma}_i$ in spin space and $\hat{\tau}_i$ in Nambu space. Together with the 2x2-identity matrix which we denote $\hat{\sigma}_0$ in spin space, the Pauli matrices form a basis for the Hilbert space of 2x2-matrices:

$$\hat{\sigma}_0 = \begin{pmatrix} 1 & 0 \\ 0 & 1 \end{pmatrix}, \hat{\sigma}_1 = \begin{pmatrix} 0 & 1 \\ 1 & 0 \end{pmatrix}, \hat{\sigma}_2 = \begin{pmatrix} 0 & -i \\ i & 0 \end{pmatrix}, \hat{\sigma}_3 = \begin{pmatrix} 1 & 0 \\ 0 & -1 \end{pmatrix}. \tag{5.4}$$

$\Psi(x)$ is a four-component spin-polarized quasiparticle state. The upper half has the dynamics of a electronlike spinor, while the lower half is effectively a holelike spinor. For a nonzero order parameter, $\hat{\Delta}(x)$, the two halves are not independent.

5.2.2 Bogoliubov-de Gennes equations

The quasiparticle propagation throughout the system is governed by the BdG-equations

$$\begin{pmatrix} \hat{H}_0(x) & \hat{\Delta}(x) \\ -\hat{\Delta}^*(x) & -\hat{H}_0^*(x) \end{pmatrix} \Psi(x) = E\Psi(x). \tag{5.5}$$

,

where $\hat{H}_0(x)$ is the single-particle Hamiltonian that remains in the case of a vanishing pairing potential and $\hat{\Delta}(x)$ is the mean-field order parameter. For s-wave pairing it takes the form $\hat{\Delta}(x) = i\hat{\sigma}_2\Delta(x)$.

The order parameter is taken to be constant in each of the superconducting regions with equal magnitude (same material), but the phase may be different in the two S regions separated by the junction. With s-wave pairing we have

$$\hat{\Delta}(x) = i\hat{\sigma}_2\Delta_0[e^{i\phi_L}\Theta(-x) + e^{i\phi_R}\Theta(x - L)] \tag{5.6}$$

We assume that the dominant contribution of the magnetic field to the energy of the ferromagnetic region is the Zeeman term so that we can neglect making the minimal substitution in the momentum operator, $\hat{p} = -i\hbar\boldsymbol{\nabla}$. The magnetization is assumed to depend only on the x-coordinate. The magnetic part of the Hamiltonian is thus

$$\hat{H}_Z(x) = -h\,\boldsymbol{\sigma}\cdot\mathbf{m}(x) \tag{5.7}$$

where $\boldsymbol{\sigma} = (\hat{\sigma}_1, \hat{\sigma}_2, \hat{\sigma}_3)$ is the Pauli vector, $\mathbf{m}(x)$ is the local magnetization direction and h represents the strength of the effective exchange field. The single-particle Hamiltonian $\hat{H}_0(x)$ changes abruptly at the interfaces:

$$\hat{H}_0(x) = \hat{H}_S[\Theta(-x)+\Theta(x-L)]+\hat{H}_F(x)\Theta(x)\Theta(L-x)+\hat{V}[\delta(x)+\delta(x-L)], \tag{5.8}$$

where $\hat{H}_S = h_S\hat{\sigma}_0$ and $\hat{H}_F = h_F\hat{\sigma}_0 + \hat{H}_Z$ with $h_{S/F} = -\frac{\hbar^2}{2m_{S/F}}\frac{\mathrm{d}^2}{\mathrm{d}x^2} - \mu_{S/F}$. We have allowed for different effective masses and Fermi energies in the ferromagnet and superconductor, distinguished by a subscript.

5.2.3 Spin-active interfaces

We model the interfaces by a δ-function potential barrier which consist of a spin-independent part of strength V_0 and spin-active part of strength ρV_0. This barrier has the form [38]

$$\hat{V} = V_0[\hat{\sigma}_0 - \boldsymbol{\rho}\cdot\boldsymbol{\sigma}] = V_0\begin{pmatrix} 1-\rho_z & -(\rho_x - i\rho_y) \\ -(\rho_x + i\rho_y) & 1+\rho_z \end{pmatrix}. \tag{5.9}$$

where $\boldsymbol{\rho}$ is a vector parallel to the magnetic moment at the interface. Its magnitude ρ effectively measures the relative importance of the spin-independent and the spin-dependent parts of the potential.

5.2.4 Boundary conditions

Charge conservation mandates continuity of the wave function which implies

$$\Psi_L(0) = \Psi_F(0) \equiv \Psi(0), \tag{5.10}$$

$$\Psi_R(L) = \Psi_F(L) \equiv \Psi(L). \tag{5.11}$$

On the other hand, the derivative of the wave function is not continuous in the case of a δ-function barrier. In order to get the appropriate boundary conditions on the derivative, we integrate the BdG-eq. (5.5).

$$\begin{aligned}
0 &= \lim_{\epsilon\to 0}\int_{-\epsilon}^{\epsilon} E\Psi(x)\mathrm{d}x = \lim_{\epsilon\to 0}\int_{-\epsilon}^{\epsilon}\begin{pmatrix}\hat{H}_0 & \hat{\Delta}\\ -\hat{\Delta}^* & -\hat{H}_0^*\end{pmatrix}\Psi(x)\mathrm{d}x\\
&= \begin{pmatrix}\hat{V} & 0\\ 0 & -\hat{V}^*\end{pmatrix}\Psi(0) + \lim_{\epsilon\to 0}\int_{-\epsilon}^{0^-}\begin{pmatrix}\hat{H}_S & \hat{\Delta}\\ -\hat{\Delta}^* & -\hat{H}_S^*\end{pmatrix}\Psi_L(x)\mathrm{d}x + \lim_{\epsilon\to 0}\int_{0^+}^{\epsilon}\begin{pmatrix}\hat{H}_F & 0\\ 0 & -\hat{H}_F^*\end{pmatrix}\Psi_F(x)\mathrm{d}x\\
&= \begin{pmatrix}\hat{V} & 0\\ 0 & -\hat{V}^*\end{pmatrix}\Psi(0) + \frac{\hbar^2}{2m_S}\lim_{\epsilon\to 0}\int_{-\epsilon}^{0^-}\begin{pmatrix}-I & 0\\ 0 & I\end{pmatrix}\Psi_L''(0)\mathrm{d}x + \frac{\hbar^2}{2m_F}\lim_{\epsilon\to 0}\int_{0^+}^{\epsilon}\begin{pmatrix}-I & 0\\ 0 & I\end{pmatrix}\Psi_F''(0)\mathrm{d}x\\
&= \begin{pmatrix}\hat{V} & 0\\ 0 & -\hat{V}^*\end{pmatrix}\Psi(0) - \frac{\hbar^2}{2m_S}\begin{pmatrix}-I & 0\\ 0 & I\end{pmatrix}\Psi_L'(0) + \frac{\hbar^2}{2m_F}\begin{pmatrix}-I & 0\\ 0 & I\end{pmatrix}\Psi_F'(0)
\end{aligned}$$

Changing the sign of the lower equations and moving the derivatives to the left-hand side results in

$$\frac{\hbar^2}{2m_F}\Psi_F'(0) - \frac{\hbar^2}{2m_S}\Psi_L'(0) = \begin{pmatrix}\hat{V} & 0\\ 0 & \hat{V}^*\end{pmatrix}\Psi(0). \tag{5.12}$$

Similarly, integration over the second interface yields

$$\frac{\hbar^2}{2m_S}\Psi_R'(L) - \frac{\hbar^2}{2m_F}\Psi_F'(L) = \begin{pmatrix}\hat{V} & 0\\ 0 & \hat{V}^*\end{pmatrix}\Psi(L). \tag{5.13}$$

5.3 Superconducting region

The solutions in either superconducting region are plane waves of the form

$$\Psi_k(x) = \begin{pmatrix} u_{k\uparrow} \\ u_{k\downarrow} \\ v_{k\uparrow} \\ v_{k\downarrow} \end{pmatrix} \mathrm{e}^{ikx} \,. \tag{5.14}$$

The effect of h_S(5.8) on the plane wave solutions is equivalent to multiplication with the kinetic energy relative the Fermi level, $\varepsilon_k = \frac{\hbar^2 k^2}{2m_S} - \mu_S$.

The BdG matrix equation (5.5) becomes

$$\begin{pmatrix} \varepsilon_k & 0 & 0 & \Delta_0 \mathrm{e}^{i\phi} \\ 0 & \varepsilon_k & -\Delta_0 \mathrm{e}^{i\phi} & 0 \\ 0 & -\Delta_0 \mathrm{e}^{-i\phi} & -\varepsilon_k & 0 \\ \Delta_0 \mathrm{e}^{-i\phi} & 0 & 0 & -\varepsilon_k \end{pmatrix} \begin{pmatrix} u_{k\uparrow} \\ u_{k\downarrow} \\ v_{k\uparrow} \\ v_{k\downarrow} \end{pmatrix} = E \begin{pmatrix} u_{k\uparrow} \\ u_{k\downarrow} \\ v_{k\uparrow} \\ v_{k\downarrow} \end{pmatrix} \tag{5.15}$$

For this system to have nontrivial solutions, we must have $E^2 = \varepsilon_k^2 + \Delta_0^2$. There are two roots for E of which only the positive one pertains to the excitations above the ground state ($E > 0$) with which we are concerned. The corresponding wave vectors have magnitude

$$k^{\pm} = k_S \sqrt{1 \pm \frac{(E^2 - \Delta_0^2)^{1/2}}{\mu_S}}, \tag{5.16}$$

where $k_S = \sqrt{2m_S\mu_S}/\hbar$ is the Fermi vector in the superconductor. The eight (non-normalized) linearly independent solutions are

$$\Psi^{\pm}_{e\uparrow}(x) = \begin{pmatrix} u\mathrm{e}^{i\phi/2} \\ 0 \\ 0 \\ v\mathrm{e}^{-i\phi/2} \end{pmatrix} e^{\pm ik^+x}, \qquad \Psi^{\pm}_{e\downarrow}(x) = \begin{pmatrix} 0 \\ ue^{i\phi/2} \\ -ve^{-i\phi/2} \\ 0 \end{pmatrix} \mathrm{e}^{\pm ik^+x}, \tag{5.17}$$

$$\Psi^{\pm}_{h\uparrow}(x) = \begin{pmatrix} ve^{i\phi/2} \\ 0 \\ 0 \\ u\mathrm{e}^{-i\phi/2} \end{pmatrix} e^{\pm ik^-x}, \qquad \Psi^{\pm}_{h\downarrow}(x) = \begin{pmatrix} 0 \\ -ve^{i\phi/2} \\ ue^{-i\phi/2} \\ 0 \end{pmatrix} e^{\pm ik^-x}, \tag{5.18}$$

where u and v are the BCS coherence factors

$$u = \sqrt{\frac{1}{2}\left[1 + \frac{(E^2-\Delta_0^2)^{1/2}}{E}\right]}, \tag{5.19a}$$

$$v = \sqrt{\frac{1}{2}\left[1 - \frac{(E^2-\Delta_0^2)^{1/2}}{E}\right]}. \tag{5.19b}$$

Above the gap, u, v and $k^{\pm}$ are real and we can write (5.19) as

$$u = \sqrt{\frac{\Delta_0}{2E}}e^{\frac{1}{2}\operatorname{arcosh}\frac{E}{\Delta_0}}, \tag{5.20a}$$

$$v = \sqrt{\frac{\Delta_0}{2E}}e^{-\frac{1}{2}\operatorname{arcosh}\frac{E}{\Delta_0}}. \tag{5.20b}$$

The solutions (5.17) represent propagating modes which carry current. Charge conservation mandates unitarity of the S-matrix. To obtain the subgap mode we can write (5.20) as

$$u = \frac{e^{\beta/2}}{\sqrt{2\cosh 2\beta}}, \quad v = \frac{e^{-\beta/2}}{\sqrt{2\cosh 2\beta}} \tag{5.21}$$

and analytically continue the parameter β to subgap energies

$$\beta = \begin{cases} \operatorname{arcosh}\frac{E}{\Delta_0}, & E > \Delta_0 \\ i\arccos\frac{E}{\Delta_0}, & E < \Delta_0 \end{cases} \tag{5.22}$$

Wave directions are defined by their group velocity

$$v_g = \frac{\partial E}{\partial \hbar k} = \frac{\varepsilon_k}{E}\frac{\hbar k}{m_S}. \tag{5.23}$$

For excitations above the ground state ($E > 0$), the waves e^{ik^+x} and e^{-ik^-x} are right-moving, whereas e^{-ik^+x} and e^{ik^-x} are left-moving.

The wave vectors (5.16) acquire imaginary parts for subgap excitations ($|E| < \Delta_0$). Such excitations must vanish in the bulk superconductor, so only the waves outgoing from the interfaces can propagate in the superconducting region. Thus the wave functions in the left (L) and right (R) regions are

$$\Psi_L(x) = a_1\Psi^-_{e\uparrow}(x) + a_2\Psi^-_{e\downarrow}(x) + a_3\Psi^+_{h\downarrow}(x) + a_4\Psi^+_{h\uparrow}(x), \tag{5.24}$$

$$\Psi_R(x+L) = b_1\Psi^+_{e\uparrow}(x) + b_2\Psi^+_{e\downarrow}(x) + b_3\Psi^-_{h\downarrow}(x) + b_4\Psi^-_{h\uparrow}(x). \tag{5.25}$$

The origin has been shifted in (5.25) to simplify the boundary equations at $x = L$. Shifting the origin simply amounts to absorbing a phase factors in the coefficients, b_i. It is understood that the phase ϕ appearing in (5.17) is different in the left and the right regions. We can write (5.24) and (5.25) more explicitly:

$$
\begin{aligned}
\Psi_L(x) =& a_1 \begin{pmatrix} u\mathrm{e}^{i\phi_L/2} \\ 0 \\ 0 \\ v\mathrm{e}^{-i\phi_L/2} \end{pmatrix} \mathrm{e}^{-ik^+x} \quad + a_2 \begin{pmatrix} 0 \\ u\mathrm{e}^{i\phi_L/2} \\ -v\mathrm{e}^{-i\phi_L/2} \\ 0 \end{pmatrix} \mathrm{e}^{-ik^+x} \\
&+ a_3 \begin{pmatrix} 0 \\ -v\mathrm{e}^{i\phi_L/2} \\ u\mathrm{e}^{-i\phi_L/2} \\ 0 \end{pmatrix} e^{ik^-x} \quad + a_4 \begin{pmatrix} v\mathrm{e}^{i\phi_L/2} \\ 0 \\ 0 \\ u\mathrm{e}^{-i\phi_L/2} \end{pmatrix} \mathrm{e}^{ik^-x} \\
\Psi_R(x) =& b_1 \begin{pmatrix} u\mathrm{e}^{i\phi_R/2} \\ 0 \\ 0 \\ v\mathrm{e}^{-i\phi_R/2} \end{pmatrix} \mathrm{e}^{ik^+(x-L)} + b_2 \begin{pmatrix} 0 \\ u\mathrm{e}^{i\phi_R/2} \\ -v\mathrm{e}^{-i\phi_R/2} \\ 0 \end{pmatrix} \mathrm{e}^{ik^+(x-L)} \\
&+ b_3 \begin{pmatrix} 0 \\ -v\mathrm{e}^{i\phi_R/2} \\ u\mathrm{e}^{-i\phi_R/2} \\ 0 \end{pmatrix} \mathrm{e}^{-ik^-(x-L)} + b_4 \begin{pmatrix} v\mathrm{e}^{i\phi_R/2} \\ 0 \\ 0 \\ u\mathrm{e}^{-i\phi_R/2} \end{pmatrix} \mathrm{e}^{-ik^-(x-L)}
\end{aligned}
$$

5.4 Ferromagnetic region

In the ferromagnetic region, the superconducting order parameter is zero so that the Schrödinger equation (5.5) for the upper and lower components of the eigenvectors, $\Psi_F(x)$, decouple.

$$
\begin{pmatrix} \hat{H}_F(x) & 0 \\ 0 & -\hat{H}_F^*(x) \end{pmatrix} \Psi_F = E\Psi_F \tag{5.26}
$$

The problem can thus be simplified by splitting the four-component $\Psi_F(x)$ into two pseudo-spinors, $\vec{f}(x)$ and $\vec{g}(x)$, describing electrons and holes[1] respectively.

[1] We refer to these states as "holes" because they obey the time-reversed Schrödinger equation

$$\Psi_F = \begin{pmatrix} \vec{f}(x) \\ \vec{g}(x) \end{pmatrix}, \text{ where } \vec{f}(x) = \begin{pmatrix} f_\uparrow(x) \\ f_\downarrow(x) \end{pmatrix} \text{ and } \vec{g}(x) = \begin{pmatrix} g_\uparrow(x) \\ g_\downarrow(x) \end{pmatrix}. \tag{5.27}$$

If $\vec{f}(x)$ is an eigenvector of the hermitian operator $\hat{H}_F(x)$ with eigenvalue E, then $\vec{f}^*(x)$ is an eigenvector of $-\hat{H}_F^*(x)$ with eigenvalue $-E$. The hole states can thus be obtained from the electron states by complex conjugating and switching the sign of the energy.

The Hamiltonian contains a Zeeman term (5.7) which depends on the magnetization. Thus, in order to find the wave function, we must first determine the shape of the domain wall. For the ferromagnet described in section 3.2, where we derived the magnetization $\mathbf{m}(x) = (\cos\varphi \operatorname{sech}(\frac{x-X}{\lambda}), \sin\varphi \operatorname{sech}(\frac{x-X}{\lambda}), \tanh(\frac{x-X}{\lambda}))^T$, we get

$$\hat{H}_Z = -h \begin{pmatrix} \tanh(\frac{x-X}{\lambda}) & \mathrm{e}^{-i\varphi} \operatorname{sech}(\frac{x-X}{\lambda}) \\ \mathrm{e}^{i\varphi} \operatorname{sech}(\frac{x-X}{\lambda}) & -\tanh(\frac{x-X}{\lambda}) \end{pmatrix}. \tag{5.28}$$

5.4.1 Trigonometric domain wall

As an approximation to the hyperbolic form in (3.11) we will consider a ferromagnetic region divided into two homogeneous domains of opposite orientations separated by a trigonometric wall. This greatly simplifies our problem as the homogeneous case is trivial and we know the trigonometric wall permits an exact expression for the wavefunction [39].

$$\mathbf{m}(x) = \begin{cases} (\cos\varphi \cos(\frac{x-X}{\lambda}), \sin\varphi \cos(\frac{x-X}{\lambda}), \sin(\frac{x-X}{\lambda}))^T, \text{ for } |x-X| < \frac{\pi}{2}\lambda \\ (0, 0, \operatorname{sgn}(x-X))^T, \text{ for } |x-X| \geq \frac{\pi}{2}\lambda \end{cases} \tag{5.29}$$

The boundaries are placed at $x = X \pm \frac{\pi}{2}\lambda$ to ensure a continuous magnetization throughout the ferromagnetic region. We note that the limit $\lambda \to \infty$ corresponds to a homogeneous magnetization in the xy-plane. We will use this as a check on our solutions.

Outside the domain wall ($|x - X| \geq \frac{\pi}{2}\lambda$) the magnetization is homogeneous parallel or anti-parallel to the z-axis and the Schrödinger equation becomes

$$\hat{H}_F \vec{f}(x) = -\left[\frac{\hbar^2}{2m_F}\frac{\mathrm{d}^2}{\mathrm{d}x^2} + \mu_F + h\,\mathrm{sgn}(x - X)\hat{\sigma}_3\right]\vec{f}(x) = E\vec{f}(x). \tag{5.30}$$

The solutions are the one-component plane waves

$$\vec{f}^{\pm}_{\uparrow}(x) = \begin{pmatrix} 1 \\ 0 \end{pmatrix} e^{\pm i q_\uparrow x}, \quad \vec{f}^{\pm}_{\downarrow}(x) = \begin{pmatrix} 0 \\ 1 \end{pmatrix} e^{\pm i q_\downarrow x}. \tag{5.31}$$

with eigenvalues

$$E_\sigma = \frac{\hbar^2 q_\sigma^2}{2m_F} - \mu_F - h\,\mathrm{sgn}(x - X)\sigma. \tag{5.32}$$

The corresponding wave vectors have magnitude

$$q_\sigma = \sqrt{\frac{2m_F}{\hbar^2}(\mu_F + E_\sigma + h\,\mathrm{sgn}(x - X)\sigma)}. \tag{5.33}$$

As the relevant energies are negligible compared to the Fermi energy, this reduces to

$$q_\sigma = \sqrt{\frac{2m_F}{\hbar^2}(\mu_F - h\,\mathrm{sgn}(x - X)\sigma)} = q_F\sqrt{1 + 2b\,\mathrm{sgn}(x - X)\sigma}, \tag{5.34}$$

where $b = h/2\mu_F$ and $q_F = \sqrt{2m_F\mu_F}/\hbar$ is the Fermi vector in the ferromagnet and $\sigma = \pm 1$ is positive for spin-up, so that on either side of the domain wall the majority spins have larger wave vector for a given energy.

Since the Hamiltonian is real, the hole states are the same as those for electrons, but with the sign of the energies switched. Since we are neglecting the energy anyway, this sign change has no effect and we can use the same basis functions for holes and electrons.

Inside the domain wall ($|x - X| < \frac{\pi}{2}\lambda$) the Zeeman term becomes

$$\hat{H}_Z = -h \begin{pmatrix} \sin(\frac{x-X}{\lambda}) & e^{-i\varphi}\cos(\frac{x-X}{\lambda}) \\ e^{i\varphi}\cos(\frac{x-X}{\lambda}) & -\sin(\frac{x-X}{\lambda}) \end{pmatrix} \tag{5.35}$$

It is useful [40] to introduce a local spin basis where the spin orientations are (anti)parallel to the local magnetization $\mathbf{m}(x)$. In this basis the Zeeman term is diagonal: $\hat{H}_Z^L = -h\hat{\sigma}_3$. The local and external bases are related by a unitary transformation

$$\begin{pmatrix} |x,\uparrow^L\rangle \\ |x,\downarrow^L\rangle \end{pmatrix} = U^T(x) \begin{pmatrix} |x,\uparrow\rangle \\ |x,\downarrow\rangle \end{pmatrix} \tag{5.36}$$

We obtain the full local Hamiltonian by a unitary transformation from the external basis

$$\hat{H}_F^L = U^\dagger \hat{H}_F U, \tag{5.37}$$

where $U(x)$ is the unitary matrix

$$U(x) = \begin{pmatrix} \cos(\frac{x-X}{2\lambda} - \frac{\pi}{4}) & e^{-i\varphi}\sin(\frac{x-X}{2\lambda} - \frac{\pi}{4}) \\ -e^{i\varphi}\sin(\frac{x-X}{2\lambda} - \frac{\pi}{4}) & \cos(\frac{x-X}{2\lambda} - \frac{\pi}{4}) \end{pmatrix}. \tag{5.38}$$

After transforming the differential operator,

$$U^\dagger \frac{\mathrm{d}^2}{\mathrm{d}x^2} U = U^\dagger \Big[U \frac{\mathrm{d}^2}{\mathrm{d}x^2} + \Big(\frac{\mathrm{d}^2 U}{\mathrm{d}x^2}\Big) + 2\Big(\frac{\mathrm{d}U}{\mathrm{d}x}\Big)\frac{\mathrm{d}}{\mathrm{d}x}\Big], \tag{5.39}$$

we obtain the local Hamiltonian

$$\hat{H}_F^L = -\frac{\hbar^2}{2m_F}\Big[\frac{\mathrm{d}^2}{\mathrm{d}x^2} - \frac{1}{4\lambda^2} + \frac{1}{\lambda}\begin{pmatrix} 0 & e^{-i\varphi} \\ -e^{i\varphi} & 0 \end{pmatrix}\frac{\mathrm{d}}{\mathrm{d}x}\Big] - \mu_F - h\,\hat{\sigma}_3. \tag{5.40}$$

The spinors we have expressed in the external basis can equivalently be expressed in the local basis:

$$\begin{aligned} |e\rangle &= f_\uparrow(x)|x,\uparrow\rangle + f_\downarrow(x)|x,\downarrow\rangle = f_\uparrow^L(x)|x,\uparrow^L\rangle + f_\downarrow^L(x)|x,\downarrow^L\rangle \\ |h\rangle &= g_\uparrow(x)|x,\uparrow\rangle + g_\downarrow(x)|x,\downarrow\rangle = g_\uparrow^L(x)|x,\uparrow^L\rangle + g_\downarrow^L(x)|x,\downarrow^L\rangle \end{aligned}$$

The change-of-basis matrix is again $U(x)$ (5.38) so that the Schrödinger equation (5.26) is still valid in the new basis:

$$\hat{H}_F^L \vec{f^L} = U^\dagger \hat{H}_F U U^\dagger \vec{f} = U^\dagger E \vec{f} = E\vec{f^L} \tag{5.41}$$

The eigenfunctions are most easily found in the local basis where (5.26) becomes

$$\begin{pmatrix} \hat{H}_F^L(x) & 0 \\ 0 & -\hat{H}_F^{L*}(x) \end{pmatrix} \begin{pmatrix} \vec{f}^L(x) \\ \vec{g}^L(x) \end{pmatrix} = E \begin{pmatrix} \vec{f}^L(x) \\ \vec{g}^L(x) \end{pmatrix}. \tag{5.42}$$

We solve the two decoupled equations separately by first making an anzats for the electron states

$$\vec{f}^L(x) = \begin{pmatrix} C_\uparrow \\ C_\downarrow \end{pmatrix} e^{iqx}, \text{ while } \vec{g}^L(x) = 0. \tag{5.43}$$

Now the Schrödinger equation becomes a simple linear algebra problem. The energies, E, and the solutions, $(C_\uparrow, C_\downarrow)^T$, are the eigenvalues and eigenvectors of the matrix

$$\begin{pmatrix} \frac{\hbar^2}{2m_F}(q^2 + \frac{1}{4\lambda^2}) - \mu_F - h & ie^{-i\varphi}\frac{\hbar^2}{2m_F}\frac{q}{\lambda} \\ -ie^{i\varphi}\frac{\hbar^2}{2m_F}\frac{q}{\lambda} & \frac{\hbar^2}{2m_F}(q^2 + \frac{1}{4\lambda^2}) - \mu_F + h \end{pmatrix}. \tag{5.44}$$

From the characteristic equation, we obtain the eigenvalues

$$E = -\mu_F + \frac{\hbar^2}{2m_F}\left(q^2 + \frac{1}{4\lambda^2}\right) \mp \sqrt{(h)^2 + \left(\frac{\hbar^2}{2m_F}\frac{q}{\lambda}\right)^2}. \tag{5.45}$$

The eigenvectors with eigenvalues (5.45) satisfy

$$\frac{C_\uparrow}{C_\downarrow} = \frac{\mp ie^{-i\varphi}(q/q_F)}{\sqrt{(q/q_F)^2 + (b/a)^2} \mp b/a}, \text{ where } a = (2\lambda q_F)^{-1},\ b = h/2\mu_F. \tag{5.46}$$

We demand that the eigenvectors be normalized according to $|C_\uparrow|^2 + |C_\downarrow|^2 = 1$, which gives

$$|C_\uparrow|^2 = \frac{1}{2}\left[1 \pm \frac{b/a}{\sqrt{(q/q_F)^2 + (b/a)^2}}\right], \quad |C_\downarrow|^2 = \frac{1}{2}\left[1 \mp \frac{b/a}{\sqrt{(q/q_F)^2 + (b/a)^2}}\right]. \tag{5.47}$$

The corresponding wave vectors are the positive and negative square roots of

$$q_\pm^2 = \frac{1}{4\lambda^2} + \frac{2m_F}{\hbar^2}\left(\mu_F + E \pm \sqrt{h^2 + \frac{\hbar^2}{2m_F}\frac{\mu_F + E}{\lambda^2}}\right). \tag{5.48}$$

We note that these wave vectors are the same as those obtained in [33] for Josephson junction with a trigonometric DW, though our notation is different. When the energy dependence is neglected, the magnitude of the wave vectors of the bound states in the domain wall are determined by characteristics of the material and can be written in terms of the Fermi wave vector and the parameters a and b defined above

$$q_\pm = q_F\sqrt{1 + a^2 \pm 2\sqrt{a^2 + b^2}}. \tag{5.49}$$

The dimensionless parameters a and b measure the relative importance of the effective exchange energy (represented by λ and h) compared to the Fermi level (represented by q_F and μ_F). They can be used to explore various limits. We first check the case of a homogeneous ferromagnet which corresponds to letting $a \to 0\,(\lambda \to \infty)$ and get back our results from the homogeneous domains: $q_\pm = q_F\sqrt{1 \pm 2b}$. The limit $b << a$ $(h\lambda << \mu_F/q_F)$ corresponds to a weak exchange field and narrow DW and yields $q_\pm = q_F\left[1 \pm a \pm \frac{b^2}{2a(1\pm a)}\right]$ and in the limit of a long DW and somewhat weak exchange $a << b << 1$, $q_\pm = q_F\sqrt{1 \pm 2b}\left[1 \pm \frac{a^2}{2b}\frac{1\pm b}{1\pm 2b}\right] \approx q_F\left[1 \pm b \pm \frac{a^2}{2b}(1 \pm b)\right]$.

From (5.47) we see that the relative phase factor between the components is $\mp i\,\mathrm{e}^{-i\varphi}\,\mathrm{sgn}(q)$. In analogy with (5.21) we write

$$|C_\sigma^\pm| = \sqrt{\frac{1}{2}\left(1 \pm \frac{b/a}{\sqrt{(q/q_F)^2 + (b/a)^2}}\right)} = \frac{\mathrm{e}^{\pm\sigma\alpha_\pm/2}}{\sqrt{2\cosh 2\alpha_\pm}},\ \alpha_\pm = \operatorname{arcosh}\sqrt{1 + \frac{q_F^2 b^2}{q_\pm^2 a^2}} \tag{5.50}$$

Now the basis of the solution space can be written

$$\frac{1}{\sqrt{2\cosh 2\alpha_s}}\begin{pmatrix} \mathrm{e}^{-i\varphi/2}\,\mathrm{e}^{s\alpha_s/2} \\ \pm si\,\mathrm{e}^{i\varphi/2}\,\mathrm{e}^{-s\alpha_s/2}\end{pmatrix}\mathrm{e}^{\pm iq_s(x-X)}, \tag{5.51}$$

where $s = \{+,-\}$ and $q_\pm$ are the positive square roots of (5.48).

The hole states can be obtained from the electron wave vectors by complex conjugating and changing the sign of the energy, E, in (5.48). Since the energies are negligible compared to the Fermi energy, the sign change has no effect and complex

conjugation is all that is needed. We are now ready to write out the full expression for the wave function inside the domain wall in the local basis: $\Psi_F^L(x) =$

$$c_1 \begin{pmatrix} e^{-i\varphi}C_\uparrow^+ \\ iC_\downarrow^+ \\ 0 \\ 0 \end{pmatrix} e^{iq_+x} + c_2 \begin{pmatrix} e^{-i\varphi}C_\uparrow^+ \\ -iC_\downarrow^+ \\ 0 \\ 0 \end{pmatrix} e^{-iq_+x} + c_3 \begin{pmatrix} e^{-i\varphi}C_\uparrow^- \\ -iC_\downarrow^- \\ 0 \\ 0 \end{pmatrix} e^{iq_-x} + c_4 \begin{pmatrix} e^{-i\varphi}C_\uparrow^- \\ iC_\downarrow^- \\ 0 \\ 0 \end{pmatrix} e^{-iq_-x} +$$
$$d_1 \begin{pmatrix} 0 \\ 0 \\ e^{i\varphi}C_\uparrow^+ \\ iC_\downarrow^+ \end{pmatrix} e^{iq_+x} + d_2 \begin{pmatrix} 0 \\ 0 \\ e^{i\varphi}C_\uparrow^+ \\ -iC_\downarrow^+ \end{pmatrix} e^{-iq_+x} + d_3 \begin{pmatrix} 0 \\ 0 \\ e^{i\varphi}C_\uparrow^- \\ -iC_\downarrow^- \end{pmatrix} e^{iq_-x} + d_4 \begin{pmatrix} 0 \\ 0 \\ e^{i\varphi}C_\uparrow^- \\ iC_\downarrow^- \end{pmatrix} e^{-iq_-x} \tag{5.52}$$

The boundary conditions (5.2.4) are expressed in the external basis. So we should identify the matrix that transforms the local wave functions into the external basis via

$$\Psi_F(x) = U_{4\text{x}4}(x)\Psi_F^L(x). \tag{5.53}$$

The Schrödinger equation in the local basis (5.42) is equivalent to its expression in the external basis (5.26) if the coordinate vectors are related by

$$\begin{pmatrix} \vec{f}(x) \\ \vec{g}(x) \end{pmatrix} = \begin{pmatrix} U(x) & 0 \\ 0 & U^*(x) \end{pmatrix} \begin{pmatrix} \vec{f}^L(x) \\ \vec{g}^L(x) \end{pmatrix}. \tag{5.54}$$

Thus, the matrix that connects the representations of the wave function in the local and external bases is

$$U_{4\text{x}4}(x) = \begin{pmatrix} c & e^{-i\varphi}s & 0 & 0 \\ -e^{i\varphi}s & c & 0 & 0 \\ 0 & 0 & c & e^{i\varphi}s \\ 0 & 0 & -e^{-i\varphi}s & c \end{pmatrix}. \tag{5.55}$$

We write $c = \cos(\frac{x-X}{2\lambda} - \frac{\pi}{4})$ and $s = \sin(\frac{x-X}{2\lambda} - \frac{\pi}{4})$ to shorten our notation. We will need the derivative of $U_{4x4}(x)$ which is

$$U'_{4x4}(x) = -\frac{1}{2\lambda}\begin{pmatrix} s & -e^{-i\varphi}c & 0 & 0 \\ e^{i\varphi}c & s & 0 & 0 \\ 0 & 0 & s & -e^{i\varphi}c \\ 0 & 0 & e^{-i\varphi}c & s \end{pmatrix}. \tag{5.56}$$

5.4.2 Local basis

We have seen the usefulness of the local spin basis for a trigonometric DW. We now use this approach on a more general DW, with the magnetization determined by the angles (θ, φ) as in (3.3). Without committing to a particular choice of φ and $\theta = \theta(x)$, we write the Zeeman term in spherical coordinates

$$\hat{H}_Z = -h\begin{pmatrix} \cos\theta & \mathrm{e}^{-i\varphi}\sin\theta \\ \mathrm{e}^{i\varphi}\sin\theta & -\cos\theta \end{pmatrix}, \tag{5.57}$$

and seek solutions to the Schrödinger equation for electrons in the ferromagnet

$$\begin{pmatrix} f''_\uparrow \\ f''_\downarrow \end{pmatrix} = -\frac{2m_F}{\hbar^2}\left(E + \mu_F + h\begin{pmatrix} \cos\theta & \mathrm{e}^{-i\varphi}\sin\theta \\ \mathrm{e}^{i\varphi}\sin\theta & -\cos\theta \end{pmatrix}\right)\begin{pmatrix} f_\uparrow \\ f_\downarrow \end{pmatrix} \tag{5.58}$$

The matrix of the Zeeman term (5.57) is hermitian for any magnetization and is diagonalizable by a unitary matrix[2]. The eigenvalues are $\pm h$ and the eigenspace has an orthonormal basis consisting the column vectors of the unitary matrix

$$U = \begin{pmatrix} e^{-i\varphi/2}\cos\frac{\theta}{2} & -e^{-i\varphi/2}\sin\frac{\theta}{2} \\ e^{i\varphi/2}\sin\frac{\theta}{2} & e^{i\varphi/2}\cos\frac{\theta}{2} \end{pmatrix}. \tag{5.59}$$

Diagonalizing (5.57) with (5.59) we get the Zeeman term in the local basis

$$\hat{H}_Z^L = U^\dagger \hat{H}_Z U = -h\hat{\sigma}_3. \tag{5.60}$$

[2]Hermitian matrices are normal.

5.4.3 Homogeneous magnetization

For a magnetization of arbitrary, but uniform direction, the kinetic operator is unaffected by the basis transformation and the local Schrödinger equation is thus

$$\frac{\mathrm{d}^2}{\mathrm{d}x^2}\begin{pmatrix} f_\uparrow^L \\ f_\downarrow^L \end{pmatrix} = -\frac{2m_F}{\hbar^2}\left(E + \mu_F + h\hat{\sigma}_3\right)\begin{pmatrix} f_\uparrow^L \\ f_\downarrow^L \end{pmatrix} \tag{5.61}$$

The solutions are one-component plane waves $(\delta_{\uparrow\sigma}, \delta_{\downarrow\sigma})^T e^{\pm iq_\sigma x}$, with dispersion

$$E_\sigma = \frac{\hbar^2 q_\sigma^2}{2m_F} - \mu_F - \sigma h, \tag{5.62}$$

where $\sigma = \{\uparrow, \downarrow\} = \{+, -\}$. The corresponding wave vectors have magnitude

$$q_\sigma = \sqrt{\frac{2m_F}{\hbar^2}(\mu_F + E_\sigma + \sigma h)} = q_F\sqrt{1 + 2b_\sigma}, \tag{5.63}$$

where $q_F = \sqrt{2m_F\mu_F}/\hbar$ is the Fermi vector in the ferromagnet and $b_\sigma = (E_\sigma + \sigma h)/2\mu_F$. Transforming with U gives the solutions in the external basis

$$\begin{pmatrix} e^{-i\varphi/2}\cos\frac{\theta}{2} \\ e^{i\varphi/2}\sin\frac{\theta}{2} \end{pmatrix} e^{\pm iq_\uparrow x}, \quad \begin{pmatrix} -e^{-i\varphi/2}\sin\frac{\theta}{2} \\ e^{i\varphi/2}\cos\frac{\theta}{2} \end{pmatrix} e^{\pm iq_\downarrow x}. \tag{5.64}$$

5.5 Conclusion

We have here set up the necessary equations to calculate the ABS energies in the ballistic limit. The next step is seemingly trivial: insert the derived form of the wavefunction into the boundary conditions, collect them all in a matrix and calculate the determinant. In reality it is not so easy as we have introduced a large set of free parameters that will complicate calculations and obscure the results. For greater transparency it will be most useful to explore a only a few effects at the time.

As mentioned in the introduction to this chapter, we have assumed an adiabatic time-evolution of the magnetization. As discussed in [41] we do not have an

explicit expression for the relaxation time, but is expected to be long, which makes the adiabatic treatment valid. In this case it will be possible to let some of the parameters of the domain wall (e.g. its center of mass) acquire a time-dependence governed by the LLG equation after having found the Andreev bound states in equilibrium.

Chapter 6

Bilayer

The simplest case of a textured ferromagnet is provided by two adjacent monodomain ferromagnets with noncolinear magnetization. For this system we can obtain analytical solutions for the ABS energies which through their contribution to the free energy, will allow us to study the interplay between the spin-polarized Josephson current and the magnetization configuration at equilibrium.

6.1 Theory

Consider a bilayer of two homogeneous ferromagnets with a relative angle θ between their magnetization vectors as shown in figure 6.1.

The equilibrium spin current $\tau = \partial F/\partial\theta$ between the layers is formally equal to a torque and similar in form to the equation for the Josephson current (4.1). Waintal and Brouwer [34] combined these two equations to obtain

$$\frac{\partial I}{\partial \theta} = \frac{2e}{\hbar}\frac{\partial \tau}{\partial \phi}, \tag{6.1}$$

which shows that the torque will depend on ϕ when the current depends on θ. As I is known to depend sensitively on θ [42, 43], the above equation shows that

the Josephson current should be able to provide a spin-transfer torque on the magnetization.

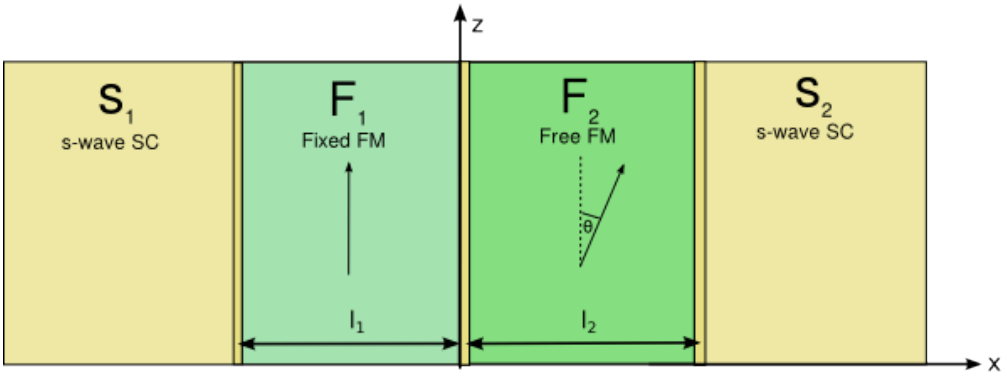

FIGURE 6.1: A bilayer of two monodomain ferromagnets with different thicknesses and anisotropy pinning, sandwiched between two singlet s-wave superconductors.

6.1.1 Model

Josephson junction consisting of two homogeneous ferromagnets sandwiched between two singlet superconducting leads (see fig. 6.1). The magnetization in the leftmost layer (F_1) is fixed perpendicular to the junction, while the magnetization in the rightmost layer (F_2) is arbitrary. The second layer must thus consist of a softer magnet, while the first layer has strong anisotropy pinning. In order to achieve a decoupling of the two layers in an experimental setting the exchange coupling between the layers could be reduced by inserting a normal metal spacer. For simplicity we ignore this and assume the barrier between the ferromagnets is perfectly transparent.

6.1.2 Andreev levels

To find the Andreev levels we first solve the BdG-equations (5.5) to obtain the eigenstates as we did in chapter 5. We assume that the effective masses are the same in all regions, while allowing different strengths for the two barriers. The

one-particle Hamiltonian (5.8) for this system takes the form

$$\hat{H}_0(x) = \Big(-\frac{1}{k_F^2}\frac{d^2}{dx^2} - 1 + \frac{Z_1}{k_F^2}\delta(x+l_1) + \frac{Z_2}{k_F}\delta(x-l_2)\Big)\mu\hat{\sigma}_0 - h\,\boldsymbol{\sigma}\cdot\mathbf{m}(x) \tag{6.2}$$

, where Z_1 and Z_2 are the normalized barrier strengths at the S/F-interfaces, h is the strength of the effective exchange field which is the same in both ferromagnets. We then collect the boundary equations into a homogeneous matrix equation and calculate the determinant using the algebraic software Maple. The calculated determinant is on the form

$$c_4(\mathrm{e}^{4\beta} + \mathrm{e}^{-4\beta}) + c_2(\mathrm{e}^{2\beta} + \mathrm{e}^{-2\beta}) + c_0, \tag{6.3}$$

where $\beta = i\arccos\frac{\varepsilon}{\Delta_0}$ as in (5.22). The energies corresponding to the eigenvalues of nontrivial solutions are found by setting the above expression equal to zero and solving for $\cos i\beta$.

$$\begin{aligned} 0 &= 2c_4\cos 4i\beta + 2c_2\cos 2i\beta + c_0 \\ &= 16c_4\cos^4 i\beta + (4c_2 - 16c_4)\cos^2 i\beta + 2c_4 - 2c_2 + c_0 \\ &\Rightarrow 8c_4\cos^2 i\beta = 4c_4 - c_2 \pm \sqrt{8c_4^2 + c_2^2 - 4c_0c_4} \end{aligned} \tag{6.4}$$

The ABS energies are then

$$\varepsilon_\pm = \Delta_0\sqrt{\frac{4c_4 - c_2}{8c_4} \pm \sqrt{\frac{8c_4^2 + c_2^2 - 4c_0c_4}{64c_4^2}}} \tag{6.5}$$

6.1.3 Free energy

The free energy is simply that of a collection of independent fermions [44], considering only excitations above the Fermi level

$$F = -2k_BT\sum_\sigma \ln 2\cosh\left(\frac{\varepsilon_\sigma}{2k_BT}\right) \tag{6.6}$$

For junctions much shorter than the superconductor coherence length, ξ, the Josephson current, $I(\phi)$, can be estimated from the discrete energy levels by using (6.6) in (4.1) which gives

$$I = -\frac{2e}{\hbar}\sum_{\sigma}\tanh\left(\frac{\varepsilon_\sigma}{2k_BT}\right)\frac{\partial\varepsilon_\sigma}{\partial\phi} \tag{6.7}$$

In general, the Josephson current, $I(\phi)$, will depend on the full quasiparticle excitation spectrum, but in the short junction regime, the continuous spectrum ($\varepsilon > \Delta_0$), does not contribute to $I(\phi)$ [45].

From the LLG equation (3.12), we see that the time-dependence of the magnetization, $\mathbf{m}$, is proportional to $\mathbf{m} \times \mathbf{H_{eff}}$. Thus in the ground state the effective field is parallel to the magnetization. As the ABS energies are independent of the azimuthal angle of the magnetization, it is the variation of the free energy with respect to the polar angle, θ, which causes an effective field perpendicular to $\mathbf{m}$, providing an effective torque

$$\frac{\partial F}{\partial\theta} = -\sum_{\sigma}\tanh\left(\frac{\varepsilon_\sigma}{2k_BT}\right)\frac{\partial\varepsilon_\sigma}{\partial\theta} \tag{6.8}$$

6.2 Results

We found the ABS energies to be of the form

$$\varepsilon_\pm = \Delta_0\sqrt{A - B\sin^2(\tfrac{\phi}{2}) \pm \sqrt{C}}, \tag{6.9}$$

where A, B and C are functions of $\cos\theta$. C is also a second degree polynomial of $\cos\phi$. In the general case of arbitrary strength of the exchange field, h, the coefficients are rather complicated and unwieldy. First we look at the case where $h = 0$ to check that in this limit our results agree with the well-known results for nonmagnetic Josephson junctions. The quantities calculated for this case are marked with the subscript zero. We then allow for a weak exchange field and

expand up to second order in the dimensionless parameter $b = h/2\mu_F$, which was introduced in (5.46).

In the absence of an exchange field, the coefficients in (6.9) reduce to

$$A_0 = 1,\ C_0 = 0,\ B_0 = (1+\zeta)^{-1}, \tag{6.10}$$

and the ABS spectrum is completely degenerate, consisting of the single energy

$$\varepsilon_0 = \Delta_0 \sqrt{\frac{\cos^2(\frac{\phi}{2}) + \zeta}{1+\zeta}}, \tag{6.11}$$

where ζ measures the effect of insulating barriers at the S/F interfaces. It is symmetric with respect to interchanging the two barriers and can be expressed as

$$\zeta = Z^2 + z^2 \sin k_F L (Z \cos k_F L + (z^2/4 - 1) \sin k_F L), \tag{6.12}$$

where Z and z are respectively the arithmetic and the geometric mean of the two barriers (see table 6.1). When the interfaces are completely transparent equation (6.11) reduces to $\varepsilon_0 = \Delta_0 \cos(\frac{\phi}{2})$, which is the familiar result for an S/N/S-junction [46]. A nonzero barrier strength ($\zeta > 0$) modifies this expression by lifting and broadening the minimum.

The Josephson current becomes

$$I_0(\phi) = -\frac{2e}{\hbar} \tanh(\frac{\varepsilon_0}{2k_B T}) \frac{\Delta_0 \sin\phi}{4\sqrt{(1+\zeta)(\cos^2(\frac{\phi}{2}) + \zeta)}}. \tag{6.13}$$

This expression is independent of θ, and vanishes when $\phi = 0$ or $\phi = \pi$. As the free energy (6.6) is strictly increasing away from zero $\varepsilon_0 = 0$, the ground state is at $\phi = 0$.

In the quasiclassical limit ($h << \mu$), the energies take on the form

$$\varepsilon_\pm = \frac{\Delta_0}{\sqrt{1+\zeta}} \sqrt{\cos^2(\tfrac{\phi}{2}) + \zeta - \mathcal{A} + \mathcal{B}\sin^2(\tfrac{\phi}{2}) - \mathcal{C}\sin^2(\tfrac{\phi}{2})\sin^2(\tfrac{\theta}{2}) + \mathcal{D}\sin^2(\tfrac{\theta}{2}) \pm \sqrt{G}}.$$

The coefficients $\mathcal{A}, \mathcal{B}, \mathcal{C}, \mathcal{D}$ and G are all of second order in $b = h/2\mu$. We use calligraphic letters for coefficients that do not depend on either ϕ nor θ, but can depend on the parameters of the junction summarized in table 6.1. G is a rather complicated expression, but can be neglected to lowest nonzero order in b when calculating the equilibrium current. While $\mathcal{A}$ and $\mathcal{B}$ depend on the total thickness of the ferromagnetic layer, L, but not on the thicknesses of the individual layers separately, $\mathcal{C}$ and $\mathcal{D}$ also depend on the relative thickness of the layers. Their expressions simplify if we also assume that the junction is short ($k_F L << 1$)

$$\mathcal{A} = \frac{2k_F^2 L^2 b^2}{(1+Z^2)^2},\ \mathcal{B} = \frac{Zk_F^2 L b^2}{(1+Z^2)^2},\ \mathcal{C} = \frac{4k_F^2 l^2 b^2 (3-Z^2)}{(1+Z^2)^3},\ \mathcal{D} = \frac{8k_F^2 l^2 b^2}{(1+Z^2)^2}, \tag{6.14}$$

The leading order term is still ε_0, which is independent of θ. Differentiating (6.14) with respect to θ gives to second order in b

$$\frac{\partial F}{\partial \theta} \approx -\tanh\left(\frac{\varepsilon_0}{2k_B T}\right) \frac{\Delta_0 \sin\theta}{4\sqrt{(1+\zeta)(\cos^2(\frac{\phi}{2})+\zeta)}} \left(\mathcal{D} - \mathcal{C}\sin^2(\tfrac{\phi}{2})\right) \tag{6.15}$$

Irrespective of ϕ, the torque vanishes when the magnetization in the free layer is parallel ($\theta = 0$) or anti-parallel ($\theta = \pi$) to the fixed-layer magnetization. Which of these is a minimum, is determined by differentiating again with respect to θ, which is trivially accomplished by replacing $\sin\theta$ with $\cos\theta$ in (6.15). We see that a stable equilibrium requires $0 > \cos\theta(\mathcal{D} - \mathcal{C}\sin^2(\frac{\phi}{2}))$. If $\mathcal{C} < \mathcal{D}$, the minimum will be at $\theta = \pi$ at irrespective of ϕ, while $\mathcal{C} > \mathcal{D}$ allows for switching the magnetization state by tuning the phase difference between the superconductors. In the transparent case, $\mathcal{C} - \mathcal{D} = 4k_F^2 l^2$, where $l = \sqrt{l_1 l_2}$ is the geometric mean of the layer thicknesses. This means that magnetization switching by a spin supercurrent should be possible in the case of a weak field and no barriers.

To see if the effect persist when the exchange is not so weak, we plot the free energy in the transparent regime as a function of ϕ and of θ in figure 6.2 for $h = \mu/5$ (i.e. $b = 0.1$). Again we find that the minimum at $\phi = 0$ and $\theta = \pi$, yet if we can make $\phi = \pi$, the minimum with respect to the magnetization configuration will switch to $\theta = 0$.

We also plot the eigenvalues (6.9) as a function of ϕ for different values of θ in figure 6.3. We see that when θ is near π, the Andreev levels become near degenerate as in the absence of spin splitting.

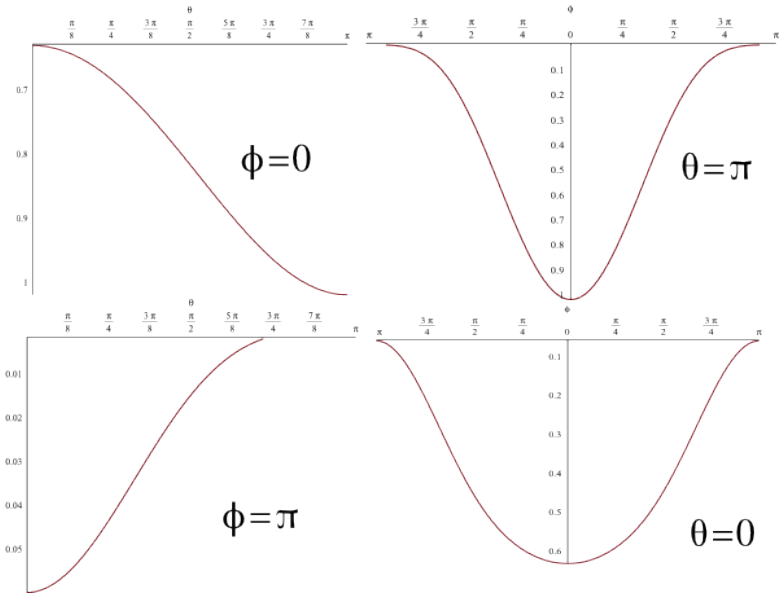

FIGURE 6.2: ABS contribution to the free energy in units of k_BT as a function of ϕ (left) and as function of θ (right) in the transparent case ($Z = 0$). We have fixed $k_FL = 10, l_1 = l_2, b = 0.1, \Delta_0 = 3k_BT/2$.

TABLE 6.1: Table of parameters of the junction and their relation to each other

symbol	definition	meaning
b	$h/2\mu$	normalized exchange field
l_1, l_2		layer thicknesses
L	$l_1 + l_2$	total thickness
l	$\sqrt{l_1 l_2}$	geometric mean
Z_1, Z_2		normalized barrier strengths
Z	$(Z_1 + Z_2)/2$	arithmetic mean
z	$\sqrt{Z_1 Z_2}$	geometric mean

6.3 Discussion

We found that for a weak field and short junction, the ground state is $\phi = 0, \theta = \pi$ and the system is essentially equivalent to an S/N/S junction. This can be understood by considering an electron and a hole propagating through the junction. If the exchange field is opposite in the two layers, the phase shifts picked up in the second layer will cancel the phase gained in the first layer. If the two layers are of equal length, the cancellation is complete and the equivalence to an S/N/S junction holds even for stronger fields [47] as we see in the case plotted in 6.3.

We have tried not to include many parameters in order to enable symbolic computation and thus obtain analytical results. Nevertheless we still have included more quantities than we have had the time to study the effects of e.g the of different layer thicknesses and different barrier strengths. Completing the study of the effects already included in the model will be the logical next step.

In future studies one may include a low but nonzero anisotropy in the soft ferromagnet to evaluate the competition between the anisotropy and ABS energies. This could be useful for identifying experimentally suitable materials.

For an arbitrary field strength and layer thicknesses, the energies can be computed, yet their form is too complicated to write down. They can still be used to analyze different limits and specific values of the parameters in addition to the transparent limit we looked at in 6.2.

We have not found a ground state with a nonzero ϕ. Yet we can still induce magnetization switching via a loop geometry and a very small external field (that does not affect the magnetization dynamics) as was suggested in [33]. In that article it was also found (for a different ferromagnetic region than the one considered here) that spin-active interfaces is important for affecting ϕ by changing the magnetization. We thus think this would be an interesting effect to add to our model.

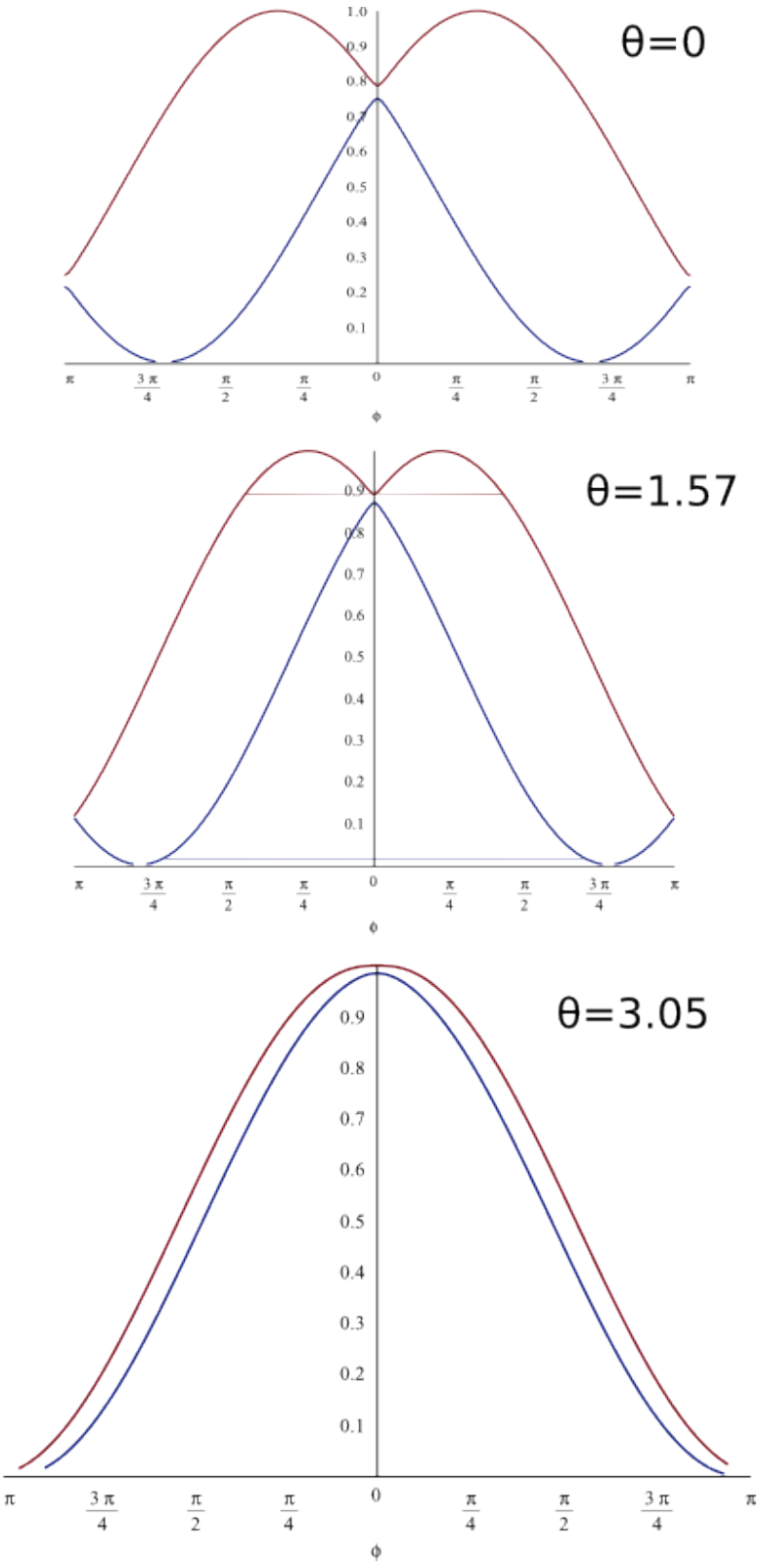

FIGURE 6.3: ABS energies Δ_0 as a function of ϕ for different values of θ in the transparent case ($Z = 0$). We have fixed $k_F L = 10, l_1 = l_2, b = 0.1$.

Chapter 7

Conclusion

We have formulated a model for investigating domain wall dynamics induced by spin supercurrents that is capable of reproducing known results in the simplest limits of homogeneous magnetization while also accommodating more complicated scenarios caused by a spatially varying bulk magnetization as well as spin mixing and rotation at the interfaces.

We then considered a simpler model consisting of a ferromagnetic bilayer sandwiched by two superconductors and showed that the superconducting phase difference can be used to switch the magnetization orientation of the free layer. Our results suggest that it is possible to use superconductors to control the ground-state configuration of magnetic spin-valves, which in turn could lead to interesting magnetoresistance-like effects [48]. These effects are of considerable interest in spintronics as they have among other things been suggested for application in magnetoresistive random access memory (MRAM) [28].

The greatest disadvantage of such a general model is that the vast parameter space makes obtaining universal results computationally intensive and even in the cases where we have been able to finish the calculation without running out of memory, the resulting expressions are cumbersome to work with.

The model can be simplified and fitted to more narrowly defined problems with a limited set of parameters which may yield more manageable expressions. The

bilayer provides a convenient case to obtain analytical results and can be analyzed further.

We have in our analysis of the bilayer system in 6 concentrated on equilibrium configuration, but with the adiabatic assumption discussed in chapter 5 the ABS contribution to the free energy can be used to consider a time-dependence of the magnetization governed by the LLG equation.

Bibliography

[1] A. I. Buzdin. Proximity effects in superconductor-ferromagnet heterostructures. *Rev. Mod. Phys.*, 77(3):935–976, September 2005. doi: 10.1103/RevModPhys.77.935. URL http://link.aps.org/doi/10.1103/RevModPhys.77.935.

[2] Dirk van Delft and Peter Kes. The discovery of superconductivity. *Physics Today*, 63(9):38–43, September 2010. ISSN 0031-9228, 1945-0699. doi: 10.1063/1.3490499. URL http://scitation.aip.org/content/aip/magazine/physicstoday/article/63/9/10.1063/1.3490499.

[3] J. Bardeen, L. N. Cooper, and J. R. Schrieffer. Theory of Superconductivity. *Phys. Rev.*, 108(5):1175–1204, December 1957. doi: 10.1103/PhysRev.108.1175. URL http://link.aps.org/doi/10.1103/PhysRev.108.1175.

[4] S. S. Saxena. Superconductivity on the border of itinerant-electron ferromagnetismin UGe_2. *Nature*, 406:587–592, 2000. doi: 10.1038/35020500.

[5] Dai Aoki, Andrew Huxley, Eric Ressouche, Daniel Braithwaite, Jacques Flouquet, Jean-Pascal Brison, Elsa Lhotel, and Carley Paulsen. Coexistence of superconductivity and ferromagnetism in URhGe. *Nature*, 413(6856):613–616, October 2001. ISSN 0028-0836. doi: 10.1038/35098048. URL http://www.nature.com/nature/journal/v413/n6856/full/413613a0.html.

[6] Igor Žutić, Jaroslav Fabian, and S. Das Sarma. Spintronics: Fundamentals and applications. *Rev. Mod. Phys.*, 76(2):323–410, April 2004. doi: 10.1103/RevModPhys.76.323. URL http://link.aps.org/doi/10.1103/RevModPhys.76.323.

[7] P. M. Tedrow and R. Meservey. Spin-Dependent Tunneling into Ferromagnetic Nickel. *Phys. Rev. Lett.*, 26(4):192–195, January 1971. doi: 10.1103/PhysRevLett.26.192. URL http://link.aps.org/doi/10.1103/PhysRevLett.26.192.

[8] P. M. Tedrow and R. Meservey. Spin Polarization of Electrons Tunneling from Films of Fe, Co, Ni, and Gd. *Phys. Rev. B*, 7(1):318–326, January 1973. doi: 10.1103/PhysRevB.7.318. URL http://link.aps.org/doi/10.1103/PhysRevB.7.318.

[9] A. Yamaguchi, S. Nasu, H. Tanigawa, T. Ono, K. Miyake, K. Mibu, and T. Shinjo. Effect of Joule heating in current-driven domain wall motion. *Applied Physics Letters*, 86(1):012511, January 2005. ISSN 0003-6951, 1077-3118. doi: 10.1063/1.1847714. URL http://scitation.aip.org/content/aip/journal/apl/86/1/10.1063/1.1847714.

[10] Jacob Linder and Jason W. A. Robinson. Superconducting spintronics. *Nat Phys*, 11(4):307–315, April 2015. ISSN 1745-2473. doi: 10.1038/nphys3242. URL http://www.nature.com/nphys/journal/v11/n4/abs/nphys3242.html.

[11] P. G. de Gennes. Boundary Effects in Superconductors. *Rev. Mod. Phys.*, 36 (1):225–237, January 1964. doi: 10.1103/RevModPhys.36.225. URL http://link.aps.org/doi/10.1103/RevModPhys.36.225.

[12] T.L. Gilbert. A phenomenological theory of damping in ferromagnetic materials. *IEEE Transactions on Magnetics*, 40(6):3443–3449, November 2004. ISSN 0018-9464. doi: 10.1109/TMAG.2004.836740.

[13] B. D. Josephson. Possible new effects in superconductive tunnelling. *Physics Letters*, 1(7):251–253, July 1962. ISSN 0031-9163. doi: 10.1016/0031-9163(62)91369-0. URL http://www.sciencedirect.com/science/article/pii/0031916362913690.

[14] A.F. Andreev. The Thermal Conductivity of the Intermediate State in Superconductors. *Sov. Phys. JETP*, 19(5):1228, 1964. URL http://www.jetp.ac.ru/cgi-bin/e/index/e/19/5/p1228?a=list.

[15] Peter Fulde and Richard A. Ferrell. Superconductivity in a Strong Spin-Exchange Field. *Phys. Rev.*, 135(3A):A550–A563, August 1964. doi: 10.1103/PhysRev.135.A550. URL http://link.aps.org/doi/10.1103/PhysRev.135.A550.

[16] A. I. Larkin and Y.N. Ovchinnikov. Inhomogeneous State of Superconductors. *Sov. Phys. JETP*, 20:762–769, 1965.

[17] W. Pauli. The Connection Between Spin and Statistics. *Phys. Rev.*, 58(8): 716–722, October 1940. doi: 10.1103/PhysRev.58.716. URL http://link.aps.org/doi/10.1103/PhysRev.58.716.

[18] M. Eschrig, T. Löfwander, T. Champel, J. C. Cuevas, J. Kopu, and Gerd Schön. Symmetries of Pairing Correlations in Superconductor–Ferromagnet Nanostructures. *J Low Temp Phys*, 147(3-4):457–476, February 2007. ISSN 0022-2291, 1573-7357. doi: 10.1007/s10909-007-9329-6. URL http://link.springer.com/article/10.1007/s10909-007-9329-6.

[19] F. S. Bergeret, A. F. Volkov, and K. B. Efetov. Odd Triplet Superconductivity and Related Phenomena in Superconductor-Ferromagnet Structures. *Reviews of Modern Physics*, 77(4):1321–1373, November 2005. ISSN 0034-6861, 1539-0756. doi: 10.1103/RevModPhys.77.1321. URL http://arxiv.org/abs/cond-mat/0506047. arXiv: cond-mat/0506047.

[20] F. S. Bergeret, A. F. Volkov, and K. B. Efetov. Manifestation of triplet superconductivity in superconductor-ferromagnet structures. *Physical Review B*, 68(6):064513, August 2003. doi: 10.1103/PhysRevB.68.064513. URL http://link.aps.org/doi/10.1103/PhysRevB.68.064513.

[21] M. Eschrig, J. Kopu, J. C. Cuevas, and Gerd Schön. Theory of Half-Metal/Superconductor Heterostructures. *Physical Review Letters*, 90(13):

137003, April 2003. doi: 10.1103/PhysRevLett.90.137003. URL http://link.aps.org/doi/10.1103/PhysRevLett.90.137003.

[22] R. S. Keizer, S. T. B. Goennenwein, T. M. Klapwijk, G. Miao, G. Xiao, and A. Gupta. A spin triplet supercurrent through the half-metallic ferromagnet CrO2. *Nature*, 439(7078):825–827, February 2006. ISSN 0028-0836. doi: 10.1038/nature04499. URL http://www.nature.com/nature/journal/v439/n7078/full/nature04499.html.

[23] Matthias Eschrig. Spin-polarized supercurrents for spintronics. *Physics Today*, 64(1):43–49, December 2010. doi: 10.1063/1.3541944. URL http://scitation.aip.org/content/aip/magazine/physicstoday/article/64/1/10.1063/1.3541944.

[24] Ya. B. Bazaliy, B. A. Jones, and Shou-Cheng Zhang. Modification of the Landau-Lifshitz equation in the presence of a spin-polarized current in colossal- and giant-magnetoresistive materials. *Phys. Rev. B*, 57(6):R3213–R3216, February 1998. doi: 10.1103/PhysRevB.57.R3213. URL http://link.aps.org/doi/10.1103/PhysRevB.57.R3213.

[25] M. Tsoi, A. G. M. Jansen, J. Bass, W.-C. Chiang, M. Seck, V. Tsoi, and P. Wyder. Excitation of a Magnetic Multilayer by an Electric Current. *Phys. Rev. Lett.*, 80(19):4281–4284, May 1998. doi: 10.1103/PhysRevLett.80.4281. URL http://link.aps.org/doi/10.1103/PhysRevLett.80.4281.

[26] E. B. Myers, D. C. Ralph, J. A. Katine, R. N. Louie, and R. A. Buhrman. Current-Induced Switching of Domains in Magnetic Multilayer Devices. *Science*, 285(5429):867–870, August 1999. ISSN 0036-8075, 1095-9203. doi: 10.1126/science.285.5429.867. URL http://www.sciencemag.org/content/285/5429/867.

[27] J. C. Slonczewski. Current-driven excitation of magnetic multilayers. *Journal of Magnetism and Magnetic Materials*, 159(1–2):L1–L7, June 1996. ISSN 0304-8853. doi: 10.1016/0304-8853(96)00062-5. URL http://www.sciencedirect.com/science/article/pii/0304885396000625.

[28] Gen Tatara, Hiroshi Kohno, and Junya Shibata. Microscopic approach to current-driven domain wall dynamics. *Physics Reports*, 468(6):213–301, November 2008. ISSN 0370-1573. doi: 10.1016/j.physrep.2008.07.003. URL http://www.sciencedirect.com/science/article/pii/S0370157308002597. 00196.

[29] V. Braude. Triplet Josephson effect with magnetic feedback in a superconductor|[ndash]|ferromagnet heterostructure. *Phys. Rev. Lett.*, 100:207001, 2008. doi: 10.1103/PhysRevLett.100.207001.

[30] Jacob Linder and Takehito Yokoyama. Supercurrent-induced magnetization dynamics in a Josephson junction with two misaligned ferromagnetic layers. *Phys. Rev. B*, 83(1):012501, January 2011. doi: 10.1103/PhysRevB.83.012501. URL http://link.aps.org/doi/10.1103/PhysRevB.83.012501. 00006.

[31] P. D. Sacramento, L. C. Fernandes Silva, G. S. Nunes, M. A. N. Araújo, and V. R. Vieira. Supercurrent-induced domain wall motion. *Phys. Rev. B*, 83(5):054403, February 2011. doi: 10.1103/PhysRevB.83.054403. URL http://link.aps.org/doi/10.1103/PhysRevB.83.054403.

[32] C. Holmqvist, S. Teber, and M. Fogelström. Nonequilibrium effects in a Josephson junction coupled to a precessing spin. *Phys. Rev. B*, 83(10):104521, March 2011. doi: 10.1103/PhysRevB.83.104521. URL http://link.aps.org/doi/10.1103/PhysRevB.83.104521.

[33] Iryna Kulagina and Jacob Linder. Spin supercurrent, magnetization dynamics, and $$\varphi${}$-state in spin-textured Josephson junctions. *Phys. Rev. B*, 90(5):054504, August 2014. doi: 10.1103/PhysRevB.90.054504. URL http://link.aps.org/doi/10.1103/PhysRevB.90.054504.

[34] Xavier Waintal and Piet W. Brouwer. Magnetic exchange interaction induced by a Josephson current. *Phys. Rev. B*, 65(5):054407, January 2002. doi: 10.1103/PhysRevB.65.054407. URL http://link.aps.org/doi/10.1103/PhysRevB.65.054407.

[35] G. E. Blonder, M. Tinkham, and T. M. Klapwijk. Transition from metallic to tunneling regimes in superconducting microconstrictions: Excess current, charge imbalance, and supercurrent conversion. *Phys. Rev. B*, 25(7):4515–4532, April 1982. doi: 10.1103/PhysRevB.25.4515. URL http://link.aps.org/doi/10.1103/PhysRevB.25.4515.

[36] M. J. M. de Jong and C. W. J. Beenakker. Andreev Reflection in Ferromagnet-Superconductor Junctions. *Phys. Rev. Lett.*, 74(9):1657–1660, February 1995. doi: 10.1103/PhysRevLett.74.1657. URL http://link.aps.org/doi/10.1103/PhysRevLett.74.1657.

[37] J. Linder and A. Sudbø. Signatures of retroreflection and induced triplet electron-hole correlations in ferromagnet s-wave-superconductor structures. *Phys. Rev. B*, 75(13):134509, April 2007. doi: 10.1103/PhysRevB.75.134509. URL http://link.aps.org/doi/10.1103/PhysRevB.75.134509.

[38] Jacob Linder, Mario Cuoco, and Asle Sudbø. Spin-active interfaces and unconventional pairing in half-metal/superconductor junctions. *Phys. Rev. B*, 81(17):174526, May 2010. doi: 10.1103/PhysRevB.81.174526. URL http://link.aps.org/doi/10.1103/PhysRevB.81.174526.

[39] Arne Brataas, Gen Tatara, and Gerrit E. W. Bauer. Ballistic and diffuse transport through a ferromagnetic domain wall. *Phys. Rev. B*, 60(5):3406–3413, August 1999. doi: 10.1103/PhysRevB.60.3406. URL http://link.aps.org/doi/10.1103/PhysRevB.60.3406.

[40] Victor A. Gopar, Dietmar Weinmann, Rodolfo A. Jalabert, and Robert L. Stamps. Electronic transport through domain walls in ferromagnetic nanowires: Coexistence of adiabatic and nonadiabatic spin dynamics. *Phys. Rev. B*, 69(1):014426, January 2004. doi: 10.1103/PhysRevB.69.014426. URL http://link.aps.org/doi/10.1103/PhysRevB.69.014426.

[41] Hyok-Jon Kwon, K. Sengupta, and Victor M. Yakovenko. Fractional ac Josephson effect in unconventional superconductors. *Low Temperature*

Physics, 30(7):613, 2004. ISSN 1063777X. doi: 10.1063/1.1789931. URL http://arxiv.org/abs/cond-mat/0401313. arXiv: cond-mat/0401313.

[42] Miodrag L. Kulić and Igor M. Kulić. Possibility of a \ensuremath{\pi} Josephson junction and switch in superconductors with spiral magnetic order. *Phys. Rev. B*, 63(10):104503, February 2001. doi: 10.1103/PhysRevB.63.104503. URL http://link.aps.org/doi/10.1103/PhysRevB.63.104503.

[43] Z. Pajović, M. Božović, Z. Radović, J. Cayssol, and A. Buzdin. Josephson coupling through ferromagnetic heterojunctions with noncollinear magnetizations. *Phys. Rev. B*, 74(18):184509, November 2006. doi: 10.1103/PhysRevB.74.184509. URL http://link.aps.org/doi/10.1103/PhysRevB.74.184509.

[44] John Bardeen, R. Kümmel, A. E. Jacobs, and L. Tewordt. Structure of Vortex Lines in Pure Superconductors. *Phys. Rev.*, 187(2):556–569, November 1969. doi: 10.1103/PhysRev.187.556. URL http://link.aps.org/doi/10.1103/PhysRev.187.556.

[45] C. W. J. Beenakker. Universal limit of critical-current fluctuations in mesoscopic Josephson junctions. *Phys. Rev. Lett.*, 67(27):3836–3839, December 1991. doi: 10.1103/PhysRevLett.67.3836. URL http://link.aps.org/doi/10.1103/PhysRevLett.67.3836.

[46] I.O. Kulik. Macroscopic Quantization and the Proximity Effect in S-N-S Junctions. *Sov. Phys. JETP*, 30(5):944, 1970. URL http://www.jetp.ac.ru/cgi-bin/e/index/e/30/5/p944?a=list.

[47] Ya. M. Blanter and F. W. J. Hekking. Supercurrent in long SFFS junctions with antiparallel domain configuration. *Phys. Rev. B*, 69(2):024525, January 2004. doi: 10.1103/PhysRevB.69.024525. URL http://link.aps.org/doi/10.1103/PhysRevB.69.024525.

[48] B. Dieny. Giant magnetoresistance in spin-valve multilayers. *Journal of Magnetism and Magnetic Materials*, 136(3):335–359, September 1994.

ISSN 0304-8853. doi: 10.1016/0304-8853(94)00356-4. URL http://www.sciencedirect.com/science/article/pii/0304885394003564.